


RESEARCH ARTICLE

WILEY

The default mode network and cognition in Parkinson's disease: A multimodal resting-state network approach

Marina C. Ruppert^{1,2}  | Andrea Greuel¹ | Julia Freigang^{1,2} | Masoud Tahmasian³ | Franziska Maier⁴ | Jochen Hammes⁵ | Thilo van Eimeren^{5,6,9} | Lars Timmermann^{1,2} | Marc Tittgemeyer^{7,8} | Alexander Drzezga^{5,9,10} | Carsten Eggers^{1,2}

¹Department of Neurology, University Hospital of Marburg, Marburg, Germany

²Center for Mind, Brain, and Behavior—CMBB, Universities of Marburg and Gießen, Marburg, Germany

³Institute of Medical Science and Technology, Shahid Beheshti University, Tehran, Iran

⁴Medical Faculty, Department of Psychiatry, University Hospital Cologne, Cologne, Germany

⁵Multimodal Neuroimaging Group, Department of Nuclear Medicine, Medical Faculty and University Hospital Cologne, University Hospital Cologne, Cologne, Germany

⁶Department of Neurology, Medical Faculty and University Hospital Cologne, University Hospital Cologne, Cologne, Germany

⁷Max Planck Institute for Metabolism Research, Cologne, Germany

⁸Cluster of Excellence in Cellular Stress and Aging Associated Disease (CECAD), Cologne, Germany

⁹German Center for Neurodegenerative Diseases (DZNE), Bonn, Germany

¹⁰Cognitive Neuroscience, Institute of Neuroscience and Medicine (INM-2), Jülich, Germany

Correspondence

Carsten Eggers, Department of Neurology, University Hospital of Giessen and Marburg, Baldingerstraße, 35033 Marburg, Germany. Email: carsten.eggers@uk-gm.de

Funding information

Deutsche Forschungsgemeinschaft, Grant/Award Number: EG350/1-1

Abstract

Involvement of the default mode network (DMN) in cognitive symptoms of Parkinson's disease (PD) has been reported by resting-state functional MRI (rsfMRI) studies. However, the relation to metabolic measures obtained by [18F]-fluorodeoxyglucose positron emission tomography (FDG-PET) is largely unknown. We applied multimodal resting-state network analysis to clarify the association between intrinsic metabolic and functional connectivity abnormalities within the DMN and their significance for cognitive symptoms in PD. PD patients were classified into normal cognition ($n = 36$) and mild cognitive impairment (MCI; $n = 12$). The DMN was identified by applying an independent component analysis to FDG-PET and rsfMRI data of a matched subset (16 controls and 16 PD patients) of the total cohort. Besides metabolic activity, metabolic and functional connectivity within the

Abbreviations: AGl, angular gyrus left; AGr, angular gyrus right; BDI-II, Beck's depression inventory version II; BNT, Boston naming test; DMN, default mode network; EPI, echo-planar imaging; FA, flip angle; FDG, Fluorodeoxyglucose; FDR, false discovery rate; FoV, field of view; fMRI, functional magnetic resonance imaging; H & Y, Hoehn and Yahr; HC, healthy controls; ICA, independent component analysis; IPL, inferior parietal lobe; LEDD, levodopa equivalent daily dose; MCI, mild cognitive impairment; NC, normal cognition; MNI, Montreal Neurological Institute; mPFC, medial prefrontal cortex; mWCST, modified Wisconsin card sorting test; PANDA, Parkinson neuropsychometric dementia assessment; ParaHL, parahippocampal cortex left; ParaHR, parahippocampal cortex right; PC, precuneus cortex; PCC, posterior cingulate cortex; PD, Parkinson's disease; PET, positron emission tomography; pSMGLs, posterior supramarginal gyrus left superior; pSMGL, posterior supramarginal gyrus left; pSMGLs, posterior supramarginal gyrus right superior; ROI, region of interest; SFGl, superior frontal gyrus left; MMSE, Mini-Mental Status Examination; midSFG, mid, superior frontal gyrus; rsfMRI, resting-state functional magnetic resonance imaging; SFGr, superior frontal gyrus right; sLOC, superior lateral occipital cortex left; sLOCr, superior lateral occipital cortex right; TE, echo time; TR, repetition time; UPDRS, unified Parkinson's disease rating scale; WMS, Wechsler memory scale.

This is an open access article under the terms of the Creative Commons Attribution-NonCommercial License, which permits use, distribution and reproduction in any medium, provided the original work is properly cited and is not used for commercial purposes.

© 2021 The Authors. *Human Brain Mapping* published by Wiley Periodicals LLC.

DMN were compared between the patients' groups and healthy controls ($n = 16$). Glucose metabolism was significantly reduced in all DMN nodes in both patient groups compared to controls, with the lowest uptake in PD-MCI ($p < .05$). Increased metabolic and functional connectivity along fronto-parietal connections was identified in PD-MCI patients compared to controls and unimpaired patients. Functional connectivity negatively correlated with cognitive composite z-scores in patients ($r = -.43$, $p = .005$). The current study clarifies the commonalities of metabolic and hemodynamic measures of brain network activity and their individual significance for cognitive symptoms in PD, highlighting the added value of multimodal resting-state network approaches for identifying prospective biomarkers.

KEYWORDS

[18F]-FDG-PET, default mode network, metabolic covariance, mild cognitive impairment, Parkinson's disease, resting-state fMRI

1 | INTRODUCTION

Mild cognitive impairment (MCI) is one of the most frequently observed nonmotor symptoms of Parkinson's disease (PD). Studies emphasize that up to 50% develop cognitive symptoms in the course of disease (Goldman et al., 2018) and the majority of PD patients with long disease duration will suffer from dementia (Hely, Reid, Adena, Halliday, & Morris, 2008). MCI may affect single or multiple cognitive domains and dramatically increases the risk for conversion to dementia (Hoogland et al., 2017). Dementia severely affects the ability to manage daily life, the patient's quality of life, mortality, and caregiver burden (Goldman, Williams-Gray, Barker, Duda, & Galvin, 2014; Levy et al., 2002). Besides enormous effort invested in the development of therapies to stop or delay cognitive decline, further research needs to be done to (a) understand neural substrates underlying cognitive impairment; (b) describe early indicators of prospective cognitive dysfunction; and (c) identify quantifiable abnormalities which could serve as objective markers to track symptom progression or the effect of interventional therapies.

Neural resting-state networks (RSNs) with importance for cognitive processing, have been examined thoroughly and reported consistently by resting-state functional MRI (rsfMRI) studies (Biswal et al., 2010). The default mode network (DMN), encompassing the precuneus cortex (PC), posterior cingulate cortex (PCC), medial prefrontal cortex (mPFC), parahippocampal cortex, and parts of the inferior parietal lobe (IPL; Raichle, MacLeod, Snyder, & Gordon, 2000), has been extensively studied in this context. Altered resting-state DMN functional connectivity has been described in neurodegenerative diseases and its prospective usefulness as imaging biomarker for cognitive dysfunction has been postulated (Hohenfeld, Werner, & Reetz, 2018). However, neurophysiological and metabolic basics of resting brain network activity and rsfMRI-derived functional connectivity remain largely unknown (Passow et al., 2015; Wehrl et al., 2013). Limited evidence suggests a close relation between resting-state functional connectivity and interregional covariance of

metabolic activity (Passow et al., 2015; Riedl et al., 2014) assessed by [18F]-fluorodeoxyglucose positron emission tomography (FDG-PET). A few recently published studies examined the topology of metabolic resting-state covariance patterns by conducting seed-based correlation or multivariate decomposition techniques such as independent component analysis (ICA) but revealed conflicting results. Particularly, some studies reported the identification of a component distinctly representing the DMN (Savio et al., 2017; Yakushev et al., 2013), whereas other studies reported weak or no metabolic correspondence of this network (Di & Biswal, 2012).

Although its basic underpinnings date back to 1984 (Clark & Stoessl, 1986; Horwitz, Grady, Schlageter, Duara, & Rapoport, 1987), the interregional analysis of metabolic activity still represents a new and rapidly evolving field. Recently, studies began to focus on metabolic connectivity—basically the interregional correlation of glucose consumption—as a marker of neuropathology and cognitive performance (Sala & Perani, 2019). Molecular FDG-PET images are likely to reveal more specific results about reflected processes, and therefore, might overcome the unspecificity of fMRI-derived functional connectivity metrics. Pioneering studies revealed characteristic changes in metabolic connectivity within defined resting-state networks in neurodegenerative diseases and its applicability as markers of cognitive dysfunction (Toussaint et al., 2012; Yakushev et al., 2013).

A large body of studies focused on resting-state networks and their prospective usefulness as imaging biomarkers of cognition in PD. Several studies reported altered resting-state functional connectivity of the DMN in PD patients with or without cognitive impairment and drew a relation to cognitive symptoms (Baggio et al., 2015; Karunanayaka et al., 2016; Lopes et al., 2017; Lucas-Jiménez et al., 2016; Tessitore et al., 2012), but findings delineating altered DMN connectivity based on rsfMRI were heterogeneous, and partly hinted at a predominant decrease or increase in functional connectivity (Amboni et al., 2015; Baggio et al., 2015; Karunanayaka et al., 2016; Krajcovicova, Mikl, Marecek, & Rektorova, 2012; Lopes et al., 2017; Tessitore et al., 2012; Zhan et al., 2018). Spetsieris

et al. (2015) concluded that DMN function is spared from pathological alterations in the early disease stage but followed by dopamine-responsive decreased metabolic connectivity in advanced stages. Using sparse-inverse covariance estimation and an interregional correlation approach, Sala et al. (2017) assessed altered metabolic connectivity in cognitively unimpaired PD patients and reported changes on multiple scales, including decreased frontal metabolic coupling in several important resting-state networks on one hand and enhanced coupling in the posterior cortex in comparison to age-matched controls on the other hand.

Given the plenty of studies which focus on single imaging modalities and fail to establish a robust marker, multimodal studies of resting-state networks are highly warranted to clarify the association between metabolic and hemodynamic network activity and its significance for cognitive dysfunction in PD. In a previous study, we reported reduced functional connectivity between the dopamine depleted putamen and DMN regions (IPL), and related metabolic changes in PD, which both were associated with global cognitive performance (Ruppert et al., 2020). No study has elaborated the correspondence between PD-associated changes in DMN metabolic network activity and functional connectivity by using FDG-PET and rsfMRI analyses in parallel. By applying a multivariate ICA-based approach followed by interregional correlation analysis to FDG-PET and rsfMRI data of healthy controls and PD patients with and without MCI, we describe consistency and differences in DMN abnormalities related to cognition in PD, obtained by cross-modal metrics in a well-characterized PD cohort.

2 | MATERIALS AND METHODS

2.1 | Subject inclusion

Twenty-five healthy controls (HC) and 60 PD patients diagnosed according to the UK Brain Bank criteria were enrolled into the study after having declared informed consent in conformation with the Declaration of Helsinki. The study was approved by the local Ethics Committee and permission was given by the Federal Office for Radiation Protection (Ethical clearance number: EK12-265). Recruitment of patients was performed via the neurological outpatient clinic at the University Hospital of Cologne and associated neurological practices. Healthy controls were recruited by word-of mouth advertising.

Subjects were excluded if one of the following exclusion criteria were met: Age < 40 years, any central nervous system diseases except for PD, and any safety concerns for MRI scanning. Particularly, patients were excluded if signs of atypical parkinsonian syndromes evolved or they had reached an advanced disease stage (i.e., Hoehn & Yahr stage >3). Dementia was excluded according to Movement Disorder Society criteria using a neuropsychological test battery with two tests for each of the five cognitive domains (Emre et al., 2007). Subjects were excluded if cognitive deficits were observed in more than one domain and severe enough to impair daily life (Emre et al., 2007).

As an additional measure of global cognitive screening, the Mini-Mental Status Examination (MMSE) was applied (Folstein, Folstein, & McHugh, 1975). In a neuropsychiatric assessment, subjects were screened for depressive symptoms by Beck's Depression Inventory version II (BDI-II; Beck, Steer, & Brown, 1996). Subjects were excluded if classified as having major depression. Participants were interviewed regarding a family history of PD or other neurodegenerative diseases. Subsets of the data analyzed in the present study were subject of previously published articles which analyzed the data in different contexts (Glaab et al., 2019; Greuel et al., 2020; Hammes et al., 2019; Ruppert et al., 2020).

2.2 | Clinical assessment

Clinical examinations were carried out at the University Hospital of Cologne, Department of Neurology. Disease severity was quantified by the Unified PD Rating Scale part III (UPDRS-III; Fahn, Elton, & UPDRS Program Members, 1987) and according to Hoehn & Yahr staging (H&Y; Hoehn & Yahr, 1967). Clinical examination and functional imaging were performed OFF-medication (12-hr [Langston et al., 1992] or 72 hr without medication in case of dopamine agonists), as it has been suggested previously (Tahmasian et al., 2015; Tahmasian et al., 2017). Levodopa-equivalent daily dose (LEDD) for total medication was calculated based on common standards (Tomlinson et al., 2010).

2.3 | Neuropsychological testing

The applied neuropsychological test battery comprised five domains: attention, memory, language, executive functions, and visuospatial abilities. At least two cognitive tests per domain were performed, including the MMSE subtests Pentagons and delayed recall, Wechsler Memory Scale (WMS) digit span test forwards and backwards (Härting & Wechsler, 2000), Parkinson Neuropsychometric Dementia Assessment (PANDA) subtests cubes and delayed recall (Kalbe et al., 2008), Regensburger verbal fluency task (alternating fluency sports-fruits, semantic fluency animals; Aschenbrenner, Tucha, & Lange, 2001), modified Wisconsin Card Sorting Test (mWCST) errors (Harris, 1990) and Boston Naming Test (BNT, (Kaplan, Googlass, & Weintraub, 1983). Individual test or subtest results were converted into standardized, age- and education-corrected domain-specific z-scores. All domain-specific z-scores were finally merged into a cognitive composite score.

Categorization of subjects into MCI and normal cognition (NC) was carried out according to Movement Disorder Society Level II criteria (Litvan et al., 2012) for all subjects who underwent both imaging modalities and complete neuropsychological assessment ($n = 16$ HC; $n = 48$ PD). Patients were diagnosed with MCI when a difference of ≥ 1.5 SD was observed in relation to age- and education-corrected norm means in at least two cognitive test results regardless of domain affiliation.

2.4 | Image acquisition and preprocessing

2.4.1 | FDG-PET

The acquisition of FDG-PET scans was conducted on an ECAT HRRT-PET-Scanner (CTI, Knoxville, TN) at the Max-Planck-Institute for Metabolism Research, Cologne. Measurements were carried out in the morning after overnight fasting and withdrawal of dopaminergic medication. Subjects were positioned along the kantho-meatal line under standardized conditions with dimmed lighting and shut eyes in a quiet room. After an initial transmission scan, 185 MBq of FDG were injected intravenously and tomographic images were dynamically acquired for 60 min. FDG-PET scans were corrected for attenuation and scattered radiation and reconstructed into one frame per 10 min with a 256×256 matrix. Resulting FDG-PET scans consisted of 207 slices with 1.22 mm voxel size. Rigid-body transformation was conducted to realign the six frames and the last four frames were finally averaged into one image for further analysis. Mean FDG-PET images were co-registered to the subject's mean fMRI-image in SPM12 (www.fil.ion.ucl.ac.uk/spm/software/spm12). Spatial normalization into Montreal Neurological Institute (MNI) space was performed by nonlinear registration to an established FDG-PET template (Della Rosa et al., 2014). Finally, FDG-PET scans were smoothed with a 6 mm full-width at half-maximum (FWHM) Gaussian kernel using SPM12.

2.4.2 | Intensity normalization

FDG-PET scans were intensity normalized using the reference cluster method, which proportionally scales each voxel with the corresponding value of a post-hoc defined reference region (Yakushev et al., 2009). In contrast to global mean normalization, it allows a more study-specific procedure to diminish inter-subject differences in intensity and has been shown to be better suited for the study of neurodegenerative diseases in which global mean differences are present (Borghammer et al., 2010; Win et al., 2019). This procedure included an initial group comparison of FDG-PET scans by voxel-wise two sample *t* test which was carried out in SPM12 with default parameters (threshold masking, proportional scaling). As mentioned elsewhere, a threshold of $t > 2$ and $p = .05$ uncorrected for multiple comparisons at voxel-level and a minimum spatial extent of 30 contiguous voxels were applied (Yakushev et al., 2009). Averaged normalized values were exported for all subjects from the cluster with the highest *t* value, in which patients exhibited an increased FDG uptake in comparison to healthy controls using the region of interest (ROI) SPM toolbox MarsBaR (Brett, Anton, Valabregue, & Poline, 2002; <http://marsbar.sourceforge.net/>, RRID:SCR_009605). Subsequently, each subject's cluster value was multiplied with the subject-specific cerebral global mean value to obtain raw values for each subject in the observed cluster. Thereafter, intensity normalization was applied to each individual's FDG-PET scan by performing proportional scaling with respect to the cluster activity using the SPM imCalc tool.

2.4.3 | Resting-state functional magnetic resonance imaging

MRI data were acquired at the Max-Planck-Institute for Metabolism Research in Cologne on a 3.0 Tesla SIEMENS MAGNETOM Prisma using the software system syngo MR D13D (Siemens, Erlangen, Germany). T1-weighted structural images were obtained with the following parameters: repetition time [TR] = 2,300 ms, echo time [TE] = 2.32 ms, flip angle [FA] = 8° , field of view [FoV] = 230 mm, slice thickness = 0.90 mm, voxel size = $0.9 \times 0.9 \times 0.9$ mm, number of slices = 192. Rs-fMRI images were acquired via a gradient-echo echo-planar imaging sequence (EPI) in interleaved acquisition mode. Acquisition parameters were as follows: slice thickness = 2 mm, FoV = 208 mm, voxel size = $2.0 \times 2.0 \times 2.0$ mm, TR = 776 ms, TE = 37.4 ms and FA = 55° . Each brain volume covered 72 axial slices; 617 acquisition time points per subject were performed.

Structural and functional MRI preprocessing and ICA were performed using SPM12 and the SPM toolbox Conn v17 (<http://www.nitrc.org/projects/conn>, RRID: SCR_009550). The default preprocessing pipeline implemented in Conn was applied, which included the following steps: functional realignment and unwarp, functional outlier detection for correction of motion artifacts (ART-based scrubbing, strict correction method according to Power, Schlaggar, and Petersen [2015]), functional and structural direct segmentation and normalization to MNI space, denoising (temporal band-pass filtering 0.01–0.1 Hz, linear detrending and further reduction of physiological noise by anatomical component-based noise correction [aCompCor; Behzadi, Restom, Liau, & Liu, 2007]) and functional smoothing (isotropic 5 mm FWHM).

2.4.4 | ICA

For the initial ICA-based identification of metabolic resting-state covariance patterns, 16 PD patients were selected from the total PD cohort for which FDG-PET and rsfMRI scans were available to match the group size of 16 HC with FDG-PET scans. This guarantees an evenly matched influence on the resulting covariance networks and improves the sensitivity for the subsequent between-group analysis (Figure 1). For ICA analysis, the single scans of 32 subjects were concatenated into one 4D file using SPM12. ICA was performed on the concatenated file using the Infomax algorithm implemented in the GIFT toolbox (<http://mialab.mrn.org/software/gift/>, RRID: SCR_001953). The number of independent components was set to 5 (Yakushev et al., 2013).

The initial ICA-based identification of fMRI resting-state networks was performed on the fMRI-data from the same sample of 32 subjects mentioned above (Figure 1). ICA was conducted by applying the Infomax algorithm implemented in the Conn toolbox. The number of independent components was set to 5. The extent of spatial overlap between both modalities' components was quantified by dice coefficient of similarity, calculated as the overlapping volume of both binary masks divided by their mean volume (Zou et al., 2004).

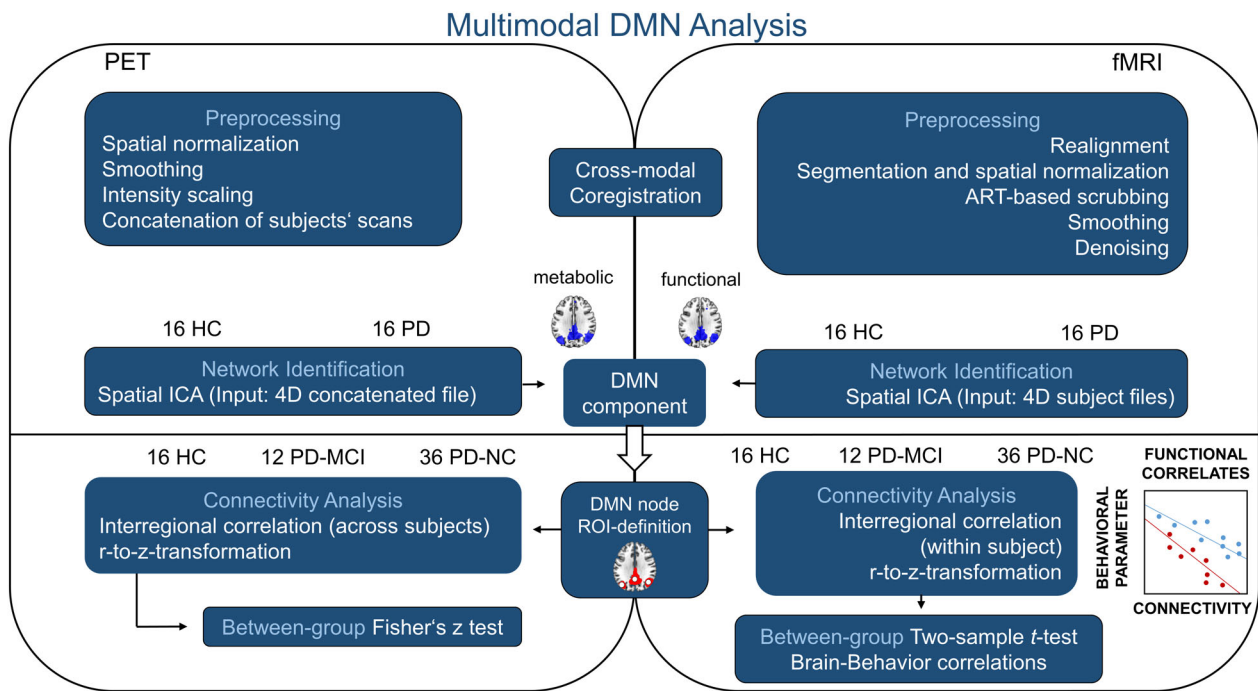


FIGURE 1 Schematic representation of the processing pipeline applied during multimodal resting-state network analysis. fMRI and FDG-PET data were preprocessed according to standard pipelines except for the intensity normalization of FDG-PET scans which followed the recently described reference cluster method. Concatenated FDG-PET scans and single subject fMRI 4D files were fed into spatial ICA with the number of components set to 5. Fifteen spherical ROIs were defined based on the resulting DMN components and interregional correlation coefficients compared between the total sample of HC, PD-NC, and PD-MCI subjects. DMN, default mode network; HC, healthy controls; ICA, independent component analysis; MCI, mild cognitive impairment; NC, normal cognition; PD, Parkinson's disease; ROI, region of interest

Figures were created using MRICroGL (<http://www.mricro.com>, RRID: SCR_002403).

2.4.5 | Cross-modal region of interest analysis

In order to compare within-network connectivity between both modalities based on interregional temporal correlation of the BOLD signal (functional connectivity) and interregional metabolic correlation (metabolic connectivity), 15 ROIs were placed within the identified DMN components (Figure 1 and Table S1). Overlapping clusters of both DMN component masks were identified by visual inspection of superimposed binary masks in MRICroGL. Spherical ROIs covering the overlapping volumes were created in MarsBaR and their position was checked by visually controlling the overlap with DMN masks. Since we were also interested in frontal DMN regions and the parahippocampal gyri have been assigned to the DMN in literature, spherical ROIs were placed in the bilateral superior frontal gyrus (SFG), mPFC, and parahippocampal clusters although they were only part of the functional component (Table S1).

Correlation coefficients for fMRI-based connectivity were obtained via conducting Pearson correlation on the mean BOLD time course of each pair of ROIs. Corresponding metabolic measures were obtained by calculating Spearman's rank correlation coefficients between the mean normalized FDG uptake of both ROIs. Extraction

of mean normalized uptake values was performed using MarsBaR. Resulting interregional correlation coefficients were z-transformed and subsequently compared between controls and PD-NC or PD-MCI patients by conducting *t*-tests in Conn (rsfMRI) or Fisher's *z* test (FDG-PET) in R (<https://www.r-project.org>).

2.5 | Statistical analyses

Statistical analyses of clinical, demographic, behavioral data, and ROI-based uptake values were performed using R. Normal distribution of numeric variables was verified by Shapiro-Wilk test. Differences between controls and the total PD group were assessed by Mann-Whitney *U* test or *t* test; differences between more than two groups by analysis of variance (ANOVA) or Kruskal-Wallis test. Post-hoc statistical analysis was carried out by performing pairwise Mann-Whitney *U* tests or *t*-tests with Bonferroni-Holm correction for multiple comparisons. Significant downward trends of FDG uptake with stronger cognitive impairment were tested one-sided by nonparametric Jonckheere-Terpstra test. An exploratory correlation analysis between imaging findings and cognition z-scores was performed in SPSS (IBM Corp. Released 2020. IBM SPSS Statistics for Windows, Version 27.0. Armonk, NY: IBM Corp) using age, sex, LEDD, UPDRS-III, disease duration, and BDI-II performance as covariates. Modulatory effects of clinical parameters on imaging results were

investigated by performing analyses of covariance (ANCOVA), including UPDRS-III, LEDD and disease duration as covariates.

2.6 | Data availability

The data set analyzed in the present study will be made available by the corresponding author upon reasonable request.

3 | RESULTS

3.1 | Subject characteristics

In total, 60 PD patients (65.02 ± 9.82 years; 19 female) and 25 healthy controls (63.52 ± 7.67 years; 13 female) were analyzed with fMRI in the current study. FDG-PET scans were available for 51 (66.45 ± 8.53 years; 18 female) of the analyzed patients and 16 healthy controls (64.63 ± 8.33 years; nine female) who underwent fMRI (Table S2). Characteristics of the 16 controls who underwent both modalities and 16 PD patients whose scans were fed into the ICA analyses are shown in Table S3.

Among the patients who underwent fMRI and FDG-PET scanning and completed neuropsychological testing, 12 patients were classified as having MCI and 36 exhibited normal cognition according to level II criteria (Litvan et al., 2012; Table 1). Six out of 36 PD-NC patients reported a family history of PD and one of the 12 PD-MCI patients mentioned a relative with PD. None of the healthy controls were categorized as having MCI and three reported a family history of PD. None of the subjects reported a family history of another

neurodegenerative disorder, aside from one PD-NC patient reporting a relative with multisystem atrophy. Demographic, clinical, and behavioral data of all subgroups are listed in Table 1. No significant differences were found among the healthy control group and patients' groups for age and gender, but for education years, BDI-II and global cognition (MMSE; Table 1). Significant differences between both patient groups were observed for MMSE, but not for education years and BDI-II. As expected, patients with MCI scored fewer points on the MMSE than PD-NC patients and healthy controls (Table 1). No significant between-group differences regarding demographic variables, motor severity and clinical measures were found between the PD-NC and PD-MCI group.

In addition, the groups differed significantly in the cognitive composite z-score and all five domain-specific z-scores (Table 2). PD-NC patients showed significantly reduced z-scores in the attention and executive domains and the cognitive composite score in comparison to controls. PD-MCI patients exhibited significantly reduced z-scores in comparison to controls and PD-NC patients in the cognitive composite score and all domains except for the language and executive domains, in which they only differed from controls (Table 2). Detailed results for all neuropsychological tests per domain and group can be found in Table 2.

3.2 | Metabolic and functional DMN components

The ICA-based analyses of concatenated FDG-PET data and fMRI data of 32 subjects revealed distinctly definable resting-state networks in both modalities. When the number of components per modality was set to 5, the DMN was the clearest visually

	FDG-PET and fMRI			
Groups	HC (n = 16)	PD-NC (n = 36)	PD-MCI (n = 12)	p value
Demographic and clinical variables				
Age, years	64.63 ± 8.33	66.69 ± 7.77	68.92 ± 8.77	.385
Gender, F/M	9/7	10 / 26	7 / 5	.060
Education, years	16.44 ± 2.06 ^{b,c}	14.44 ± 2.77 ^a	13.82 ± 2.75 ^a	.018*
DD, years	–	4.61 ± 3.68	4.13 ± 2.20	.838
UPDRS III total	–	24.67 ± 9.13	23.25 ± 7.00	.943
H & Y, stage (n)	–	2 (22) 2.5 (9) 3 (5)	2 (6) 2.5 (5) 3 (1)	.530
LEDD	–	410.48 ± 231.81	519.63 ± 181.62	.107
MMSE	28.94 ± 1.00 ^c	29.03 ± 0.88 ^c	26.50 ± 2.47 ^{a,b}	.001***
BDI-II	3.47 ± 6.00 ^{b,c}	8.86 ± 5.70 ^a	9.83 ± 7.61 ^a	<.001***

Note: Between-group differences were analyzed by ANOVA, Kruskal–Wallis test, Student's *t*-test or Mann–Whitney *U* test, and for dichotomous variables by Chi-square test. Significant post-hoc test results in comparison to *a* = HC, *b* = PD-NC, or *c* = PD-MCI are indicated by superscripts.

Abbreviations: BDI-II, Beck's depression inventory; DD, disease duration; H&Y, Hoehn and Yahr; HC, healthy controls; LEDD, Levodopa equivalent daily dose; PD-MCI, PD patients with mild cognitive impairment; PD-NC, PD patients with normal cognition; MMSE, mini-mental status examination.

p* < .05; *p* < .01; ****p* < .001.

TABLE 1 Demographic, clinical, and behavioral characteristics of PD patients with and without cognitive impairment and controls included in the multimodal cohort

TABLE 2 Neuropsychological characteristics of PD patients with and without cognitive impairment and controls included in the multimodal cohort

	FDG-PET and fMRI			
Groups	HC (n = 16)	PD-NC (n = 36)	PD-MCI (n = 12)	p value
Scores for individual neuropsychological subtests				
Visuospatial				
MMSE pentagons	0.26 ± 0.00 ^c	0.04 ± 0.91 ^c	−2.69 ± 1.78 ^{a,b}	<.001***
PANDA cubes	0.09 ± 1.14	0.15 ± 1.02 ^c	−0.68 ± 1.04 ^b	.044*
Language				
Semantic fluency	1.20 ± 0.54 ^{b,c}	0.45 ± 0.85 ^a	0.18 ± 0.91 ^a	.002**
Boston naming test	0.19 ± 0.35	0.04 ± 0.47	−0.07 ± 0.53	.359
Executive function				
mWCST errors	0.22 ± 0.74 ^{b,c}	−0.59 ± 0.50 ^{a,c}	−1.03 ± 0.73 ^{a,b}	<.001***
Alternating fluency	1.04 ± 0.95 ^{b,c}	0.37 ± 0.83 ^a	0.13 ± 1.19 ^a	.025*
Attention				
Digit span forwards	1.03 ± 0.76 ^{b,c}	−0.14 ± 0.97 ^a	−0.40 ± 1.13 ^a	<.001***
Digit span backwards	0.28 ± 1.18 ^c	−0.18 ± 0.81	−0.65 ± 0.87 ^a	.039*
Memory				
Delayed recall PANDA	−0.04 ± 1.12 ^c	−0.60 ± 1.43	−2.20 ± 2.56 ^a	.024*
Delayed recall MMSE	0.28 ± 0.95	0.40 ± 0.83	−0.31 ± 1.05	.097
Neuropsychological z-scores				
Cognitive composite score	0.46 ± 0.32 ^{b,c}	−0.01 ± 0.30 ^{a,c}	−0.80 ± 0.35 ^{a,b}	<.001***
Visuospatial	0.18 ± 0.57 ^c	0.10 ± 0.74 ^c	−1.69 ± 0.87 ^{a,b}	<.001***
Language	0.70 ± 0.32 ^c	0.29 ± 0.65	0.01 ± 0.68 ^a	.010*
Executive function	0.63 ± 0.58 ^{b,c}	−0.11 ± 0.53 ^a	−0.45 ± 0.75 ^a	<.001***
Attention	0.65 ± 0.87 ^{b,c}	−0.14 ± 0.71 ^{a,c}	−0.53 ± 0.90 ^{a,b}	<.001***
Memory	0.12 ± 0.85 ^c	−0.10 ± 0.89 ^c	−1.26 ± 1.44 ^{a,b}	.010*

Note: Between-group differences were analyzed by ANOVA or Kruskal–Wallis test; pairwise Student's *t* test or Mann–Whitney *U* tests were performed for post-hoc comparisons. Significant post-hoc test results in comparison to *a* = HC, *b* = PD-NC, or *c* = PD-MCI are indicated by superscripts.

Abbreviations: HC, healthy controls; MMSE, Mini-Mental Status Examination; mWCST, modified Wisconsin Card Sorting Test; PANDA, Parkinson Neuropsychometric Dementia Assessment, PD-MCI, PD patients with mild cognitive impairment; PD-NC, PD patients with normal cognition.

p* < .05; *p* < .01; ****p* < .001.

recognizable resting-state network in both modalities. In the fMRI data set, the other four components represented either the visual, fronto-parietal, dorsal-attention, or sensorimotor network. In the FDG-PET data set, a sensorimotor component with subcortical contribution, an auditory network, a midline cingulate cortex component with parietal clusters (Di & Biswal, 2012) and one noise component representing CSF noise were identified. The spatial correspondence between the metabolic and the fMRI DMN component was fair (dice coefficient = 0.25). But, especially for posterior DMN regions including the PC, PCC, and the bilateral superior lateral occipital cortex (sLOC) higher correspondence was observed (dice coefficient = 0.27; Figure 2). Nevertheless, some regions were found to be part of the functional DMN component, but not of the metabolic one or vice versa. The most striking differences were found in the frontal cortex, where frontal areas involving the frontal pole, frontal medial cortex, paracingulate gyrus, and subcallosal cortex were found to be part of the fMRI component but absent in the FDG-PET component (Figure 2). Further, clusters in the SFG which extended into the

juxtapositional lobule were found in both modalities, but only in the metabolic component additional clusters in the anterior cingulate gyrus and paracingulate gyrus were found to be part of the network. Additionally, the bilateral parahippocampal gyri were part of the functional network but not reported in the corresponding metabolic pattern. Parts of the cerebellar cortex were obtained in the metabolic covariance pattern but not in the functional component, and the parietal cluster extended into the cuneal cortex and occipital pole in the metabolic component (Figure 2). Similar findings were observed when ICA was performed on the fMRI data of 25 controls and 25 patients (Figure S1).

3.3 | Metabolic DMN activity is decreased in PD-NC patients and further decreases with MCI

When normalized FDG uptake values were exported from 15 ROIs placed within the identified DMN components and compared

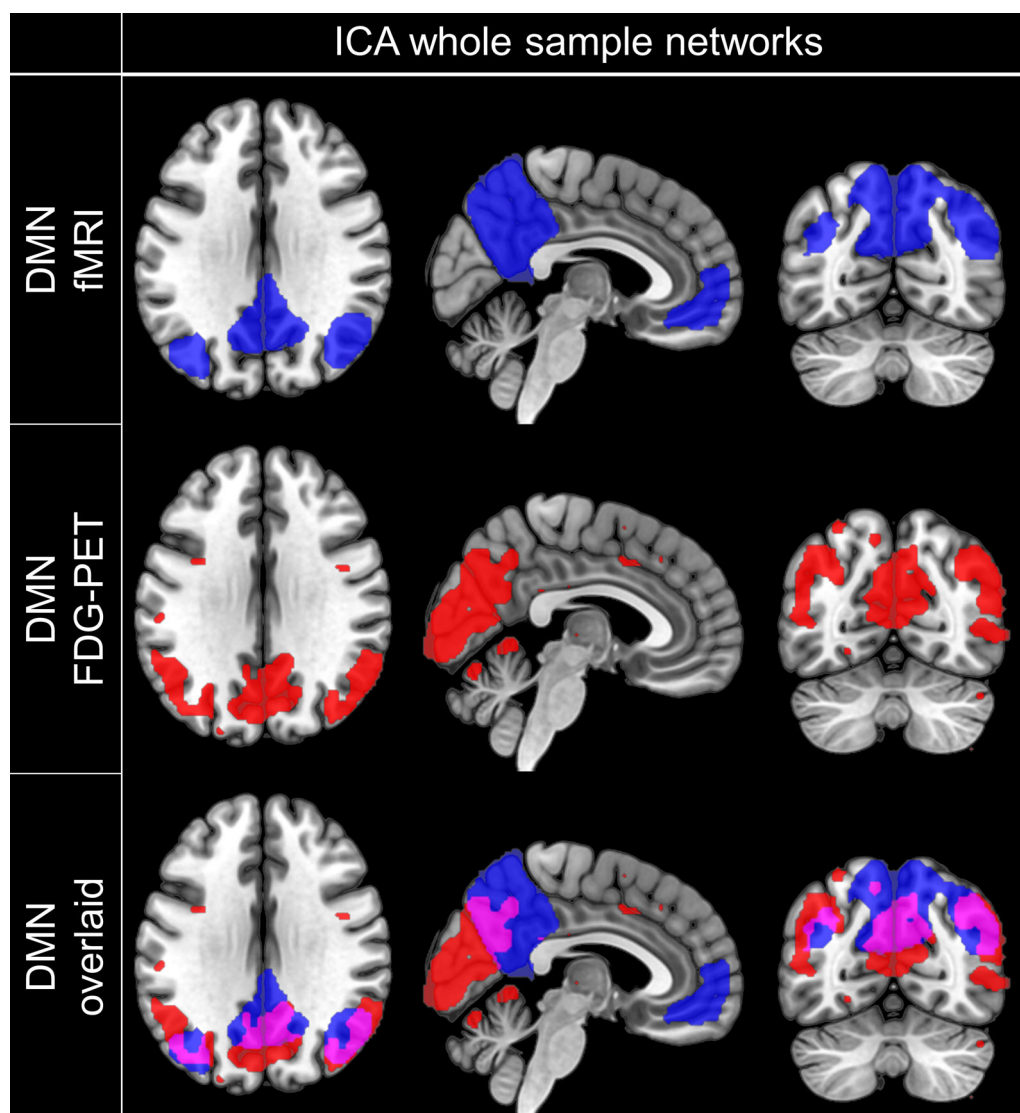


FIGURE 2 Spatial coincidence of ICA-derived metabolic and functional DMN. Spatial distribution of components representing the DMN obtained by fMRI (first row) or FDG-PET (second row) and their spatial correspondence (third row). Masks were created by thresholding the component-specific group maps at $z = 2$ and overlaid on a T1-weighted MNI template for visualization. Neurological view. DMN, default mode network; ICA, independent component analysis; FDG-PET, Fluorodeoxyglucose positron emission tomography

between healthy controls, cognitively normal patients and patients with MCI, significant differences in metabolic activity were identified between the groups for all ROIs (Figure 3, Kruskal-Wallis test, $p < .05$, Table S4). For all DMN regions, a significant trend towards an increment of metabolic deficits from healthy controls via unimpaired patients to patients with MCI was identified (Figure 3, Jonckheere-Terpstra test; $p < .01$, Table S4). The identified trend, which indicated stronger metabolic deficits with increasing cognitive impairment remained significant after controlling for UPDRS-III scores, disease duration and LEDD in patients (Table S4). The most profound metabolic deficits between both patient groups and healthy controls were found in the PC (pairwise Wilcoxon test; HC vs. PD-NC difference in location: 0.17 [0.10; 0.25] $p < .001$ (all p values Bonferroni-Holm adjusted); HC versus PD-MCI: 0.24 [0.17; 0.36] $p < .0001$, the right

posterior superior supramarginal gyrus (pSMGr; HC vs. PD-NC: 0.20 [0.10; 0.27] $p < .0001$; HC vs. PD-MCI: 0.22 [0.10; 0.34] $p = .001$) and right superior lateral occipital cortex (sLOC; HC vs. PD-NC: 0.16 [0.09; 0.23] $p < .0001$; HC vs. PD-MCI: 0.22 [0.15; 0.31] $p < .0001$) as well as the right angular gyrus (AGr; HC vs. PD-NC: 0.18 [0.09; 0.27] $p < .001$; HC vs. PD-MCI: 0.26 [0.16; 0.38] $p < .001$). Although the decreasing trend was significant, visual inspection of mean FDG uptake values revealed that for some regions only minor between-group differences were found between cognitively unimpaired and impaired patients, especially for ROIs that were exclusively found to be part of the network in the fMRI analysis but not the FDG-PET component (mPFC, parahippocampal cortex left [ParaHL], parahippocampal cortex right [ParaHR], and superior frontal gyrus right [SFGr]).

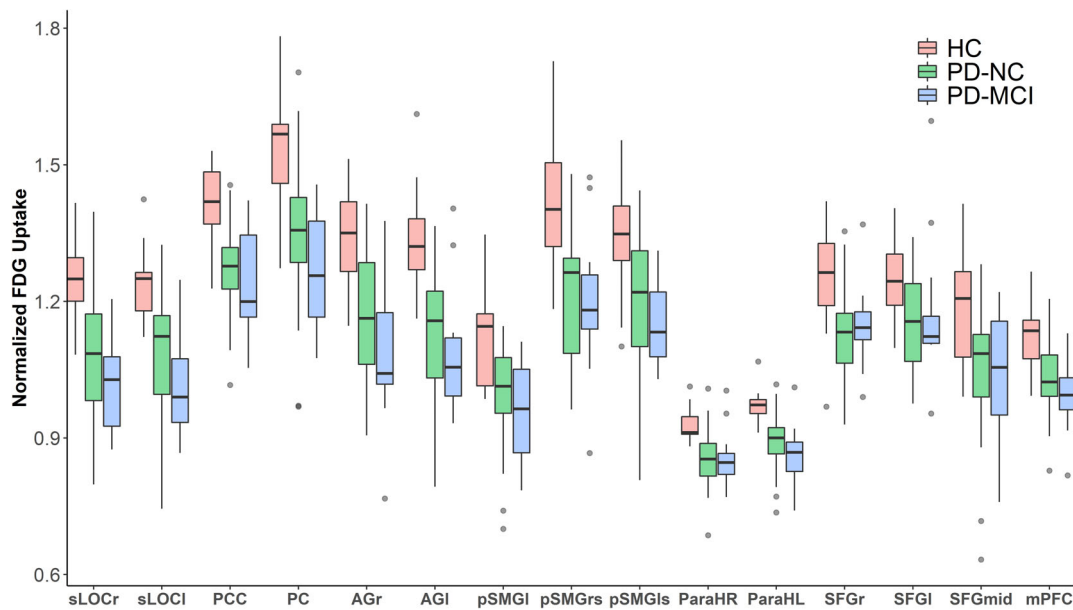


FIGURE 3 Metabolic DMN activity in HC ($n = 16$), PD-NC ($n = 36$), and PD patients with MCI ($n = 12$). In PD patients, normalized regional FDG uptake was significantly reduced in all DMN nodes when compared to healthy controls. For all ROIs, a significant trend towards a progressive metabolic deficit from healthy controls via cognitively unimpaired patients to MCI patients was observed (Jonckheere–Terpstra test $p < .01$). Grey colored dots indicate outliers (defined as >1.5 times the interquartile distance range). AGI, angular gyrus left; AGr, angular gyrus right; HC, healthy controls; mPFC, medial prefrontal cortex; ParaHL, parahippocampal cortex left; ParaHR, parahippocampal cortex right; PC, precuneus cortex; PCC, posterior cingulate cortex; PD-MCI, PD patients with mild cognitive impairment; PD-NC, PD patients with normal cognition; pSMGI, posterior supramarginal gyrus left; pSMGLs, posterior supramarginal gyrus left superior; pSMGrs, posterior supramarginal gyrus right superior; SFGI, superior frontal gyrus left; SFG mid, superior frontal gyrus mid; SFGGr, superior frontal gyrus right; sLOCI, superior lateral occipital cortex left; sLOCr, superior lateral occipital cortex right

3.4 | Metabolic connectivity is altered in PD-NC and changes proceed in PD-MCI

An exploratory analysis of interregional metabolic connectivity between DMN ROIs revealed gradually changing differences in network coherency between healthy controls and the groups of cognitively unimpaired and impaired PD patients. Patients with normal cognition exhibited an increased metabolic connectivity between the SFGGr and posterior DMN regions, especially the AGr ($z = 2.61$, p value = .009; Figure 4a). These changes were also found in patients with MCI compared to HC and the reported differences were of stronger magnitude in this patient group, especially for the AGr ($z = -3.56$, p value $<.001$), the posterior division of the left superior supramarginal gyrus (pSMGLs; $z = -2.13$, p value = .033), and the left superior occipital cortex (sLOCI; $z = -2.03$, p value = .043; Figure 4b). Patients with MCI further showed a significantly higher correlation between the SFGGr and the PC ($z = -2.13$, p value = .033) compared to unimpaired patients (Figure 4c). In addition to this increase along fronto-parietal connections, an increased correlation of regional metabolic activity was observed between posterior DMN regions in both patient groups compared to healthy controls (Figure 4a,b). Cognitively normal and impaired patients showed a trend towards an increased metabolic connectivity between the AGr and the sLOCr compared to controls (PD-NC: $z = -3.02$, $p = .003$; PD-MCI: $z = -1.57$, $p = .116$);

patients with MCI additionally between the PC and sLOCr ($z = -2.02$, p value = .043; Figure 4a,b). In addition, patients without cognitive impairment exhibited a significantly increased metabolic connectivity between the ParaHL and posterior DMN regions, especially the left posterior supramarginal gyrus (pSMGI; $z = 2.57$, p value = .010) and sLOCI ($z = 2.42$, p value = .015). The latter observations were not observed in patients with MCI (Figure 4a,b). By contrast, in patients with MCI decreased metabolic connectivity was found between the ParaHR and mostly posterior DMN regions, including the pSMGI ($z = 2.48$, p value = .013) and left angular gyrus (AGI; $z = 2.01$, p value = .045), in comparison to cognitively unimpaired patients (Figure 4c).

3.5 | Posterior and fronto-parietal functional hyperconnectivity proceeds in PD-MCI

A comparison of interregional hemodynamic correlations among 15 ICA-derived DMN ROIs between the three groups revealed primarily an increase of functional connectivity along fronto-parietal connections in cognitively impaired patients compared to unimpaired patients and healthy controls. In patients without MCI, an increased functional connectivity between the PC and the sLOCI was observed in comparison to controls (Figure 5a-1, $p_{\text{uncorr}} = .041$). Patients with

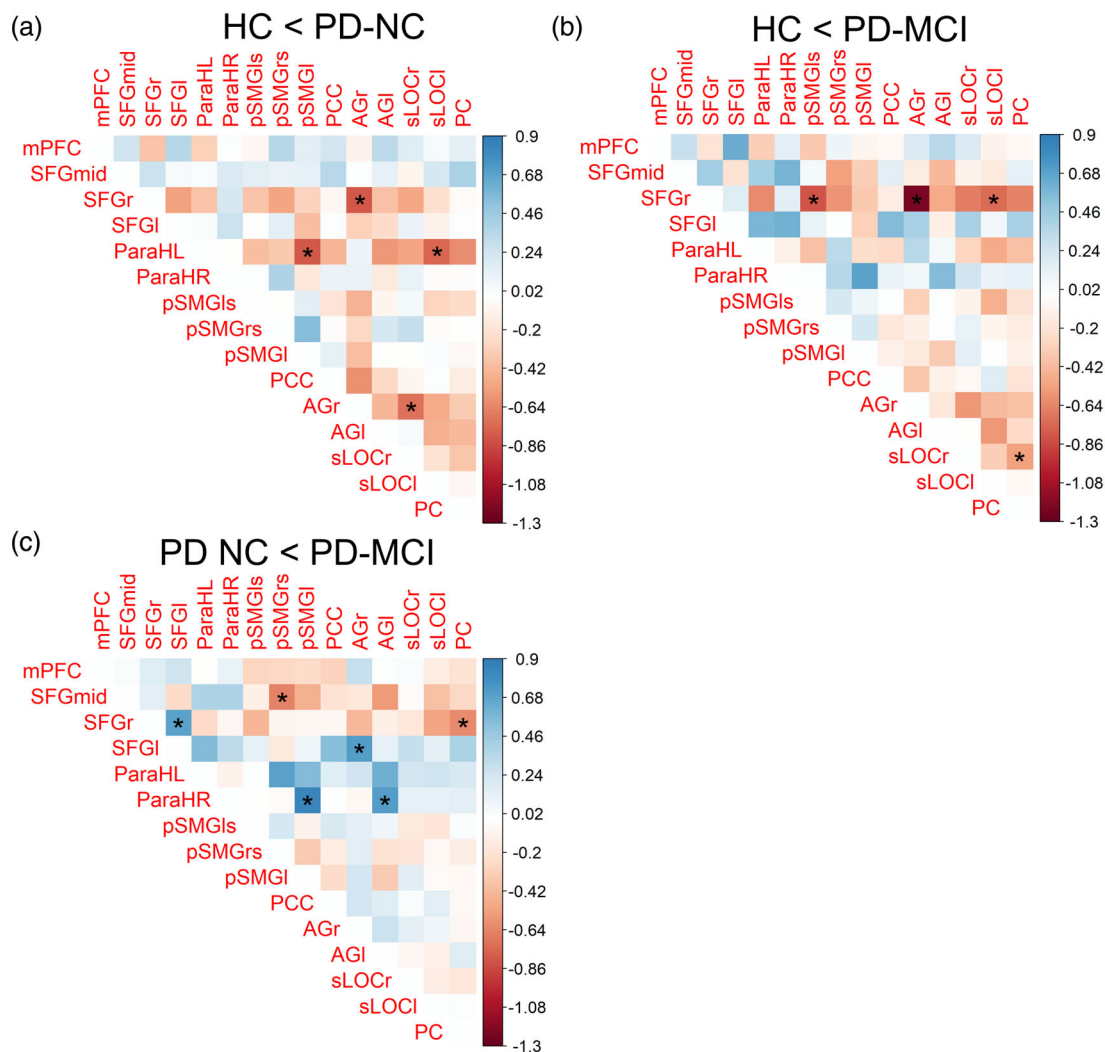


FIGURE 4 Group differences in metabolic connectivity of DMN ROIs between healthy controls and cognitively impaired (PD-MCI) or unimpaired (PD-NC) PD patients. Color scale indicates the difference in correlation coefficients between the groups. Correlation coefficients were compared by Fisher's z test; *significant at $p < .05$. AGI, angular gyrus left; AGr, angular gyrus right; mPFC, medial prefrontal cortex; ParaHL, parahippocampal cortex left; ParaHR, parahippocampal cortex right; PC, precuneus cortex; PCC, posterior cingulate cortex; PD-MCI, PD patients with mild cognitive impairment; PD-NC, PD patients with normal cognition; pSMGI, posterior supramarginal gyrus left; pSMGls, posterior supramarginal gyrus left superior; pSMGrS, posterior supramarginal gyrus right superior; SFGI, superior frontal gyrus left; SFG mid, superior frontal gyrus mid; SFGGr, superior frontal gyrus right; sLOCI, superior lateral occipital cortex left; sLOCr, superior lateral occipital cortex right

normal cognition further showed decreased functional connectivity of the AGr and the PCC ($p_{FDR} = 0.013$), ParaHL and the left superior frontal gyrus (SFGI; $p_{uncorr} = .024$), and between both the AGI ($p_{uncorr} = 0.046$) and the pSMGrS ($p_{uncorr} = .043$) and the ParaHR compared to controls (Figure 5a-1 and Table 3). In addition, functional connectivity between the SFGGr and both, the PCC ($p_{uncorr} = .011$) and AGr ($p_{FDR} = .047$) was reduced in PD-NC patients compared to controls. In patients with cognitive impairment, increased functional connectivity was additionally found between the SFGI and the PC ($p_{uncorr} = .043$) and between the pSMGls and SFGGr ($p_{uncorr} = .005$) as well as between the mPFC and both the AGr and SFGI compared to controls (Figure 5a-2, $p_{uncorr} < .05$). Reductions of functional connectivity were found in PD-MCI patients compared to controls between the pSMGrS and SFGI ($p_{uncorr} = .033$).

A direct comparison of DMN ROI-based connectivity among both patient groups revealed an increased functional connectivity in MCI patients between each of the following ROIs: PC, right AG, and PCC (Figure 5a-3 and Table 3). In addition, the PC was correlated stronger with the ParaHL ($p_{uncorr} = .013$), the PCC with the mPFC ($p_{uncorr} = .021$) and the AGr with the SFGI ($p_{FDR} = .030$) in patients with MCI (Figure 5a-3 and Table 3). The reported differences among both patient groups remained significant after controlling for UPDRS-III, disease duration and LEDD (Figure S3). No significant decreases of functional connectivity were observed in patients with MCI compared to patients with normal cognition among DMN regions. Similar findings were observed when group differences were analyzed in a larger rsfMRI sample which had not undergone FDG-PET scanning (Figure S2).

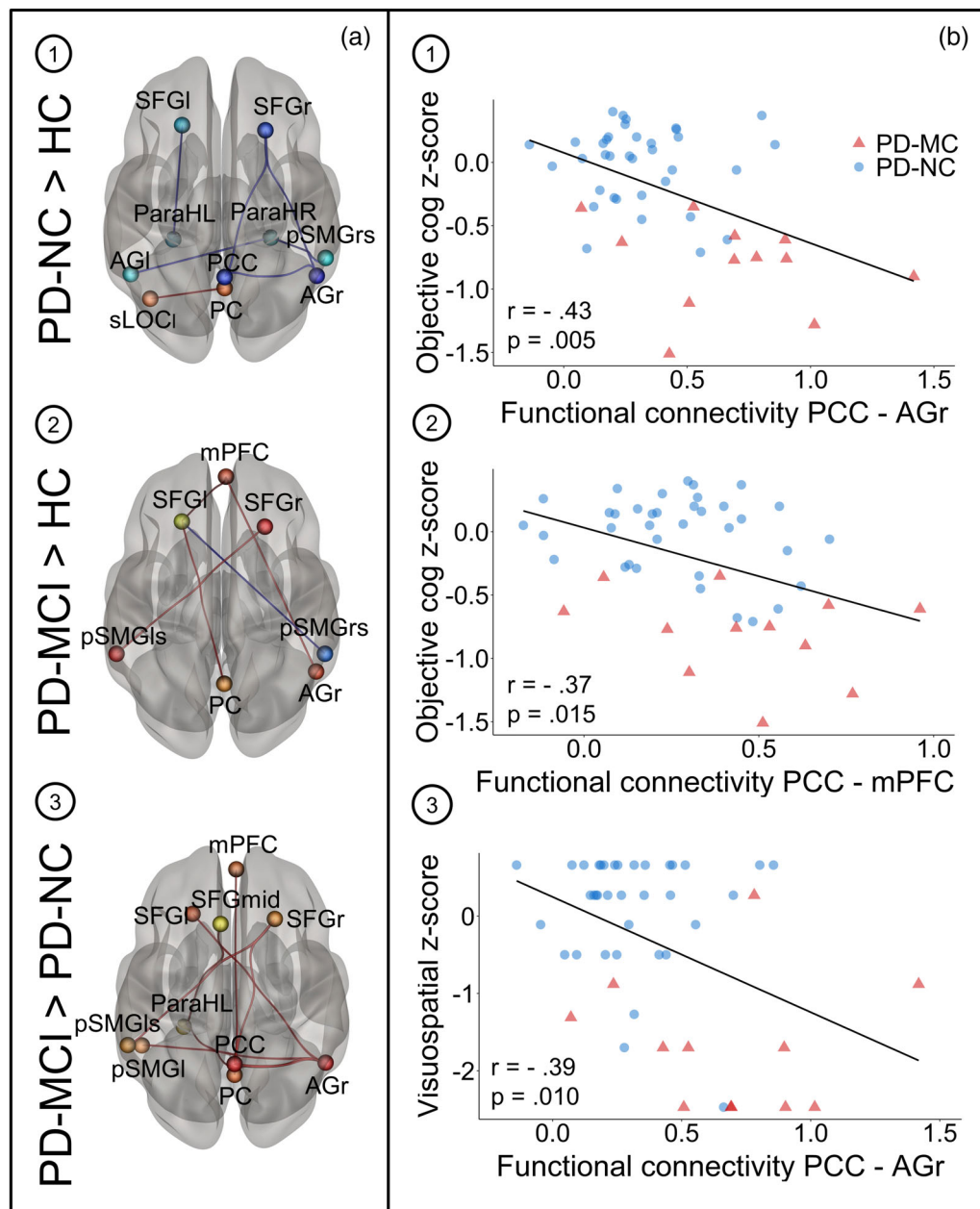


FIGURE 5 (a) Group differences in functional connectivity of DMN ROIs between healthy controls ($n = 16$) and cognitively impaired ($n = 13$) and unimpaired ($n = 36$) PD patients. Between-group differences were tested two-sided with threshold set at p uncorrected or FDR-corrected $< .05$. Connections shown in red represent increased connectivity strength, blue connections refer to the opposite contrast. ROIs' sizes do not indicate the actual ROI diameters. Results are shown in 3D view from superior perspective. Neurological view. (b) Correlation plots showing significant negative correlations between functional connectivity and cognitive z-scores in PD patients for the following connections and z-scores: (1) PCC-AGr and cognitive composite z-scores, (2) PCC-mPFC and cognitive composite z-scores and (3) PCC-AGr and visuospatial z-scores. Pearson's correlation coefficients and p values are shown on the bottom left in each plot. AGI, angular gyrus left; AGr, angular gyrus right; mPFC, medial prefrontal cortex; ParaHL, parahippocampal cortex left; ParaHR, parahippocampal cortex right; PC, precuneus cortex; PCC, posterior cingulate cortex; PD-MCI, PD patients with mild cognitive impairment; PD-NC, PD patients with normal cognition; pSMGI, posterior supramarginal gyrus left; pSMGls, posterior supramarginal gyrus left superior; pSMGrs, posterior supramarginal gyrus right superior; SFGI, superior frontal gyrus left; SFG mid, superior frontal gyrus mid; SFGGr, superior frontal gyrus right; sLOCi, superior lateral occipital cortex left; sLOCr, superior lateral occipital cortex right

3.6 | DMN hyperconnectivity is associated with cognitive impairment in PD patients

An exploratory partial correlation analysis between domain-specific cognitive z-scores, metabolic activity and functional connectivity

revealed significant negative associations between DMN functional connectivity and cognitive composite z-scores as well as positive associations between DMN metabolic activity and cognitive composite z-scores in patients. Cognitive composite z-scores correlated significantly with functional connectivity between the (a) PCC and AGr

TABLE 3 Statistics of ROI-based functional connectivity analysis between healthy controls ($n = 16$) and cognitively impaired ($n = 12$) and unimpaired PD patients ($n = 36$)

Contrast and regions	tstatistic	p_{uncorr}	p_{FDR}
PD-MCI > PD-NC			
Seed AGr			
PCC	4.27	.0001	.0013
SFGI	3.00	.0043	.0301
PC	2.47	.0172	.0725
pSMGI	2.40	.0207	.0725
Seed PCC			
AGr	4.27	.0001	.0013
PC	2.89	.0059	.0411
SFGr	2.53	.0149	.0696
mPFC	2.39	.0210	.0733
Seed PC			
PCC	2.89	.0059	.0803
ParaHL	2.58	.0131	.0803
AGr	2.47	.0172	.0803
Seed mPFC			
PCC	2.39	.0210	.2934
Seed SFGI			
AGr	3.00	.0043	.0603
Seed SFGr			
PCC	2.53	.0149	.1868
pSMGIs	2.29	.0267	.1868
Seed pSMGIs			
SFGr	2.29	.0267	.3736
ParaHL			
PC	2.58	.0131	.1838
SFGmid	2.13	.0386	.2699
Seed pSMGI			
AGr	2.40	.0207	.2899
Seed SFG mid			
ParaHL	2.13	.0386	.5399
PD-NC > HC			
Seed AGr			
PCC	-3.51	.0010	.0134
SFGr	-3.08	.0034	.0237
Seed SFGI			
ParaHL	-2.33	.0237	.3320
Seed PC			
sLOCI	2.10	.0411	.5366
Seed PCC			
AGr	-3.51	.0010	.0134
SFGr	-2.63	.0113	.0791
Seed SFGr			
AGr	-3.08	.0034	.0474
PCC	-2.63	.0113	.0791

TABLE 3 (Continued)

Contrast and regions	tstatistic	p _{uncorr}	p _{FDR}
Seed ParaHL			
SFGl	−2.33	.0237	.2725
Seed AGl			
ParaHR	−2.05	.0457	.6404
Seed sLOCl			
PC	2.10	.0411	.4504
Seed ParaHR			
pSMGrS	−2.07	.0434	.3202
AGl	−2.05	.0457	.3202
PD-MCI > HC			
Seed AGr			
mPFC	2.23	.0349	.3307
Seed pSMGls			
SFGr	3.08	.0048	.0678
Seed SFGl			
mPFC	2.46	.0208	.2005
PC	2.13	.0430	.2005
pSMGrS	−2.25	.0334	.2005
Seed SFGr			
pSMGls	3.08	.0048	.0678
Seed PC			
SFGl	2.13	.0430	.4733
Seed mPFC			
SFGl	2.46	.0208	.2445
AGr	2.23	.0349	.2445
Seed pSMGrS			
SFGl	−2.25	.0334	.4680

Abbreviations: AGl, angular gyrus left; AGr, angular gyrus right; FDR, false discovery rate; mPFC, medial prefrontal cortex; ParaHL, parahippocampal cortex left; ParaHR, parahippocampal cortex right; PC, precuneus cortex; PCC, posterior cingulate cortex; PD-MCI, PD patients with mild cognitive impairment; PD-NC, PD patients with normal cognition; pSMGl, posterior supramarginal gyrus left; pSMGls, posterior supramarginal gyrus left superior; pSMGrS, posterior supramarginal gyrus right superior; SFGl, superior frontal gyrus left; SFG mid, superior frontal gyrus mid; SFGr, superior frontal gyrus right; sLOCl, superior lateral occipital cortex left; sLOCr, superior lateral occipital cortex right.

($r = -.43$, $p = .005$, Figure 5b-1), (b) PCC and mPFC ($r = -.37$, $p = .015$, Figure 5b-2), and (c) AGr and SFGl ($r = -.32$, $p = .040$) when controlling for age, sex, LEDD, UPDRS-III, disease duration, and BDI-II. Visuospatial z-scores also showed a significant linear association with the functional connectivity between the AGr and PCC ($r = -.39$, $p = .010$, Figure 5b-3) and the connectivity between the AGr and SFGl ($r = -.33$, $p = .032$). A negative association was identified between the attention domain z-scores and the functional connections PC-PCC ($r = -.32$, $p = .037$) and ParaHL-PC ($r = -.33$, $p = 0.034$). By contrast, only the executive domain z-scores correlated positively with metabolic activity, especially in the sLOCl ($r = .50$, $p = .001$), sLOCr ($r = .33$, $p = .031$), PC ($r = .36$, $p = .019$), SFGl ($r = .36$, $p = .019$), pSMGls ($r = .55$, $p < .001$), and AGl ($r = .31$, $p = .042$). No significant correlation was observed between functional connectivity and UPDRS-III scores, LEDD or disease duration. In posterior DMN regions (pSMGrS, AGl,

AGr, pSMGls, and sLOCr) and SFGl metabolic activity negatively correlated with disease severity, quantified by UPDRS-III, LEDD, and disease duration.

4 | DISCUSSION

In the current study, we applied a multivariate ICA approach on both fMRI and FDG-PET data of healthy controls and PD patients with and without MCI to study consistency and differences in DMN abnormalities related to cognitive symptoms in PD. Post-hoc ROI-based analyses were performed to unravel the relation between local glucose consumption, interregional metabolic and functional connectivity in controls and a well-characterized PD cohort. Particularly, we opened new perspectives by clarifying if disease related changes in functional

connectivity within the DMN are accompanied by similar changes in metabolic connectivity and associated with metabolic deficits in PD patients with and without MCI. In contrast to previous analysis in this cohort, we focused on the comprehensive neuropsychological data, methodologically applied a completely data-driven ICA approach to FDG-PET and rsMRI data to obtain study-specific DMN components and performed interregional metabolic analyses.

In line with PETMRI hybrid studies in healthy controls, we found a fair spatial correspondence of the DMN in resting-state FDG-PET and fMRI data in the analyzed subjects, with higher spatial convergence in parieto-occipital regions. Focusing on DMN metabolic activity, we encountered a gradual metabolic decline in all DMN ROIs, with strongest metabolic deficits in the posterior DMN in PD-MCI. By integrating both modalities, we provide first evidence for a predominant increase in hemodynamic and metabolic network coherency between posterior DMN regions, including the PC, AG, and the sLOC and the frontal cortex in cognitively impaired patients compared to unimpaired patients and healthy controls. Fronto-parietal interregional correlations revealed by both modalities were elevated in unimpaired patients and proceeded (i.e., further increased) in cognitively impaired patients, while reduced connectivity of the parahippocampal gyri in PD-MCI was exclusively observed in the PET modality. Increased functional connectivity along fronto-parietal connections and in the posterior DMN was significantly associated with worse cognitive functions in PD patients.

The present study partly continues, and answers questions raised in response to our previous study, which hinted at an involvement of DMN regions in cognitive symptoms of PD and a relation between functional network degeneration and metabolic activity (Ruppert et al., 2020). The current study for the first time clarifies the commonalities of both measures of brain network activity and their individual significance for cognitive symptoms in PD. Our results highlight how multimodal resting-state studies can provide new insights into the (patho-)physiological network organization of brain activity by confirming insights obtained with one modality but also how multimodal approaches can deepen our understanding of disease processes.

4.1 | Spatial convergence of metabolic and hemodynamic DMN

In the current study, fair spatial correspondence was detected between metabolic covariance across subjects and coherent hemodynamic fluctuations within the DMN in a subset of 16 healthy controls and 16 PD patients. These observations stand in accordance with a previous hybrid scanner study which reported a moderate spatial convergence between metabolic covariance and fMRI-derived DMN patterns in simultaneously acquired data sets of 22 healthy, mid-aged subjects (Savio et al., 2017). Interestingly, Savio et al. (2017) found similar differences between the FDG-PET- and fMRI-derived DMN: prefrontal clusters were smaller in the FDG-PET modality but included more medial frontal regions, and parts of the cerebellar cortex were only found with FDG-PET (Figure 2). In line with the present findings,

Di and Biswal (2012) described only posterior DMN regions in an FDG-PET ICA, while the medial prefrontal cortex was included in the corresponding fMRI DMN component. In contrast, by conducting a comparable ICA (GIFT, five components) in 35 mid-aged healthy subjects, Yakushev et al. (2013) observed the typical DMN topology in FDG-PET data with extensive involvement of the prefrontal cortex. The fact that a similar spatial overlap can be identified in independently or simultaneously acquired images and across different age ranges supports the hypothesis that metabolic networks, characterized by common covariance across subjects, can robustly be detected in the resting human brain. This underscores the assumption that, at least in posterior parts of the DMN, synchronous hemodynamic fluctuations at rest are a result of coherent neural activity. Residual differences in network distribution between both modalities might be related to the overall different methodology of network identification by using static FDG-PET data (one image per subject) or fMRI-data (image timeseries per subject). The selection of included FDG-PET frames and further parameters of the acquisition protocol (e.g., time spent after radioligand injection) might also have a critical influence on network analysis and might provoke discrepancies among different studies.

4.2 | Reduced FDG uptake in DMN ROIs is associated with network-level changes in PD

Here, we report significantly reduced FDG uptake in all DMN regions in patients with normal cognition and a significant trend towards a progressive decline in PD-MCI patients. The observation of frontal and occipito-parietal hypometabolism in PD-MCI compared to patients with normal cognition stands in accordance with previous studies emphasizing parietal, occipital, temporal and frontal metabolic decreases as classical features observed in PD-MCI (Hosokai et al., 2009; Huang et al., 2008; Lyoo, Jeong, Ryu, Rinne, & Lee, 2010; Pappatà et al., 2011), which further progress in PD dementia (Garcia-Garcia et al., 2012) and are independent from medicative status (Pappatà et al., 2011). In addition, comparable studies report similar but limited metabolic changes in patients with normal cognition compared to healthy controls (Garcia-Garcia et al., 2012; Hosokai et al., 2009; Huang et al., 2008; Pappatà et al., 2011).

Interestingly, regions in which the strongest metabolic deficits and gradual decline were observed in comparison to controls (PC, sLOCr, AGr, and pSMGr), mainly including the posterior DMN, also showed the strongest increases in both metabolic and functional connectivity, indicating a link between degenerative processes on one hand and network reorganization on the other hand. All these regions were found to be part of both the metabolic covariance pattern and the fMRI component. By contrast, in regions which showed only a minor difference in glucose metabolism between patient groups (e.g., ParaHR), a reduced metabolic connectivity was found in patients with MCI compared to both healthy controls and unimpaired patients. Further, the latter regions were also not identified as parts of the metabolic DMN component.

4.3 | Metabolic and functional network alterations in the posterior DMN in PD with and without cognitive impairment

When functional and metabolic connectivity within the DMN were compared between healthy controls and both groups of PD patients, several similarities between both measures of coherent network activity were identified. In both modalities, PD patients with and without MCI in their OFF-state exhibited an increased correlation between frontal and posterior DMN regions in comparison to controls. Increased functional connectivity, for example, between the SFG and pSMGs, was accompanied by similar changes in metabolic connectivity in PD-MCI compared to controls. By contrast, decreased metabolic correlation was observed between the PC and the left SFG, but functional connectivity was increased in PD-MCI compared to controls. Although significantly increased functional connectivity was observed between the AGr and PCC in PD-MCI compared to PD-NC, no increased metabolic correlation was detected between these regions. On the other hand, while strikingly decreased metabolic covariance of the ParaHR with the pSMG and AGI was observed in PD-MCI compared to PD-NC, no decreased functional connectivity was noticed.

The increased interregional metabolic correlations in posterior DMN regions in PD patients detected here stand in accordance with observations from Sala et al. (2017) who reported enhanced metabolic coupling in the posterior cortex in PD patients with normal cognition compared to age-matched controls. Additionally, Baggio et al. (2015) revealed an increased functional correlation between the DMN and posterior cortical regions, including the bilateral dorsal precuneus, posterior cingulate gyrus, and superior occipital areas involving the occipito-parietal junctions in PD patients with and without cognitive impairment compared to controls. Of note, the authors found a significant negative association between these functional connectivity alterations and visuospatial performance in PD (Baggio et al., 2015). In the current study, we observed a significant increase in functional connectivity along fronto-parietal connections in PD-MCI compared to PD-NC and healthy controls and a comparable association between the functional connectivity of the PC, PCC, and mPFC and objective cognition in PD patients. Similarly, Zhan et al. (2018) reported an increased functional connectivity between the PCC and the bilateral mid frontal gyri, middle temporal gyrus, left precuneus, and posterior cerebellum in cognitively impaired PD patients compared to unimpaired patients. An rsfMRI study of early PD patients by Caso et al. (2013) also revealed an increased connectivity within DMN regions, including the temporal gyri, hippocampus and parahippocampus, precuneus, and the cingulate cortices in comparison to healthy controls. The latter findings seem to contradict previous rsfMRI studies, which report decreased functional connectivity of DMN regions, for example, the IPL, medial-temporal lobe and precuneus, but contrary to our study, most of the studies which reported decreased DMN functional connectivity in PD-MCI analyzed patients in their ON-state (Amboni et al., 2015; Lucas-Jiménez et al., 2016). Dopaminergic impact on DMN activity has been reported by previous studies (Krajcovicova et al., 2012) and a few studies

hinted at a modulatory role of dopamine which contributes to decreases in DMN connectivity (Conio et al., 2020). Further, the decreased metabolic connectivity between frontal regions belonging to the DMN component observed in our study is in line with findings by Sala et al. (2017), who revealed reduced frontal metabolic coupling in several important resting-state networks in PD.

By integrating both measures of network coherency and local glucose metabolism, it becomes clear that DMN dysfunction—characterized by increased connectivity between frontal and parietal regions—and concurrent local metabolic deficits represent a PD-related phenomenon occurring in the absence of cognitive impairment. The occurrence of MCI is not solely explained by more profound local metabolic changes but accompanied by additional alterations in network parameters. In particular, strongly decreased metabolic connectivity is evident between the parahippocampal areas and the parietal cortex, and stronger fronto-parietal synchronization is identified with both modalities at this stage. Previous studies suggested that decreased metabolic connectivity in the frontal cortex and occipital hyperconnectivity might have compensatory effects in cognitively unimpaired PD patients (Sala et al., 2017). By contrast, functional connectivity within the posterior DMN and fronto-parietal synchronization further increased with worse cognitive functioning in PD-MCI in the present cohort. It could thus be speculated that increased posterior synchronization represents a contributor for cognitive impairment rather than a compensatory mechanism for cognitive function in PD patients. In support of this hypothesis, Gardini et al. (2015) speculated that an increased functional connectivity between the PCC and the medio-temporal lobe, which they observed in MCI patients, might represent a maladaptive response to neurodegenerative processes, for example, atrophy.

This corresponds with recently published longitudinal studies of cortical thinning in PD, which report reduced cortical thickness in occipital and parietal lobes in PD patients with normal cognition and additional thinning of frontotemporal regions in cognitively impaired patients (Filippi et al., 2020; Gorges et al., 2020). In PD patients with conversion to MCI, cortical thinning was observed in the precuneus and posterior cingulum, medial and superior frontal gyri, and supramarginal gyri (Filippi et al., 2020), key regions of the DMN for which dysregulated network connectivity was observed in the present study. In line with the first appearance of hippocampal metabolic dysconnectivity and increasing frontoparietal connectivity alterations at the MCI stage reported here, Filippi et al. (2020) highlight structural changes of the hippocampus and fronto-temporo-parietal regions as key drivers of cognitive impairment. Gorges et al. (2020) provide evidence of cortical thinning in anterior DMN regions in baseline MRI scans of PD patients who developed cognitive impairment compared to patients who remained cognitively stable. Cortical thinning confined to the anterior cingulate cortex was associated with cognitive performance and may be an early predictor of future cognitive impairment (Gorges et al., 2020) and the aforementioned functional imbalance in PD. At some point, the imbalance induced by fronto-parietal synchronization and parahippocampal desynchronization proceeds and normal cognition can no longer be maintained. The increased

coherent DMN activity in PD patients in the OFF-state reported in the current study may be related to the inability to deactivate during cognitive tasks described by previous studies (Ibarretxe-Bilbao et al., 2011; van Eimeren, Monchi, Ballanger, & Strafella, 2009), which has also been linked to poor cognitive performance (Gardini et al., 2015).

Further studies including patients with PD dementia are required to resolve whether hyperconnectivity represents a phenomenon contributing to cognitive decline (Baggio et al., 2015) or maintaining cognitive function. In line with the increased metabolic connectivity within posterior cortical regions reported in the present study, including the SMG, sLOC and AG, Toussaint et al. (2012) also reported an increase in correlated metabolic activity between parietal and temporal hypometabolic regions in MCI patients with conversion to AD compared to controls. Another similarity between both studies is the increased correlation between frontal and parietal regions which was more pronounced in PD-MCI or MCI converters. Toussaint et al. (2012) found this alteration to break down during transition from MCI to AD. Another study reported increased metabolic correlation strength in the dorsal DMN in older subjects and less elevated measures in ApoE ϵ 4 carriers or amyloid positive subjects with higher risk of suffering from AD (Arnemann, Stöber, Narayan, Rabinovici, & Jagust, 2018). Together with the current findings, it can be speculated that decreased metabolic activity and reorganization towards an increased coherent activity within posterior DMN regions might precede the clinical manifestation of MCI.

It is still an open question if there is a relation between cortical hypometabolism, network alterations, and PD pathology. For example, dopaminergic imaging studies reveal evidence for an involvement of striato-frontal pathway degeneration in frontal dysfunction (Hammes et al., 2019; Polito et al., 2012). Additionally, there might be a possible link between posterior cortical dysfunction and the degeneration of cholinergic pathways (Hilker et al., 2005; Klein et al., 2010). Particularly, volumetric studies of longitudinally obtained t1-weighted MRI scans revealed evidence for a role of basal forebrain cholinergic nuclei in the development of cognitive decline in PD (Ray et al., 2018). Since preliminary findings show a modulatory role of the basal forebrain for DMN activity (Nair et al., 2018), there might be a possible link to DMN dysregulation reported in the current study. Future studies, combining comprehensive analyses of multiple neurotransmitter systems, are highly warranted to complete our knowledge about network dysfunction in the PD spectrum.

4.4 | Limitations and future directions

A limitation of the current study is the low number of controls which may restrain the identification of more significant differences between healthy controls and patients. Another critical point represents the fact that metabolic covariance studies focusing on static FDG-PET images are restricted to group-level analysis, resulting in one correlation measure per group in contrast to fMRI analysis, where interregional correlations can be assessed on a subject level. Since FDG-PET connectivity

measures are therefore quite rough and critically depend on the cohorts' homogeneity in image acquisition and preprocessing, the good spatial correspondence of multimodally obtained resting-state networks is remarkable. Further studies should combine dynamic FDG-PET acquisitions with fMRI to assess within-subject glucose dynamics. Recent investigations in animal models have shown the usefulness of constant infusion protocols in this context (Amend et al., 2019). Additionally, decreased metabolic connectivity in frontal regions of patients might have contributed to the fact that not all frontal regions were represented in the PET-DMN component. However, including only one group in the initial pattern derivation would have introduced bias for subsequent analysis. The patient groups examined in the current study did not differ in disease duration, motor impairment, LEDD and mood status. Therefore, it can be assumed that differences in cognitive performance were also not substantially driven by depressive mood. Finally, simultaneous acquisition of both modalities using hybrid PETMRI scanners would enable a more direct comparison of metabolic and functional resting brain activity. However, the adherence of standard conventions regarding subject instruction, scanner environment and cross-modal registration in the current study enabled a sufficient intra- and inter-subject comparability. Since there is mounting evidence that impairment of posterior cortical regions precedes cognitive symptoms (Williams-Gray et al., 2009), the present findings should be confirmed in longitudinal studies.

5 | CONCLUSION

To date, comprehensive studies that compare both functional and metabolic resting-state connectivity across subjects within the same PD cohort were still lacking, although combining modalities could complement the insights obtained with one modality and provide greater diagnostic accuracy. By performing interregional analysis in two modalities, we describe a spatial association between patterns of altered functional and metabolic DMN connectivity in PD patients with distinctly defined cognitive profiles in comparison to controls. While univariate FDG uptake was gradually reduced in PD patients, with PD-MCI patients showing the lowest metabolism in all DMN nodes, increased interregional metabolic and functional connectivity along fronto-parietal connections was found in PD-MCI compared to controls and unimpaired patients. Therefore, the data are suggestive of a relation between hypometabolism and network reorganization in cognitive decline, since they provide evidence for proceeding metabolic deficits and network synchrony within the DMN, associated with poorer cognitive performance. The current study for the first time clarifies the commonalities of both measures of brain network activity and their individual significance for cognitive symptoms in PD, highlighting the added value of multimodal resting-state network approaches for identifying prospective biomarkers.

ACKNOWLEDGMENTS

This study received funding by the Deutsche Forschungsgemeinschaft (DFG) in context of the Clinical Research Group 219 (KFO

219, EG350/1-1). The authors would like to thank all participants who made the current work possible and colleagues who were involved in data acquisition. Open Access funding enabled and organized by Projekt DEAL.

CONFLICT OF INTEREST

The authors declare no conflicts of interest.

ETHICS STATEMENT

The study was approved by the local Ethics Committee of the University of Cologne and permission was given by the Federal Office for Radiation Protection (Ethical clearance number: EK12-265).

DATA AVAILABILITY STATEMENT

The data set analysed in the present study will be made available by the corresponding author upon reasonable request.

ORCID

Marina C. Ruppert  <https://orcid.org/0000-0002-9025-7058>

REFERENCES

- Amboni, M., Tessitore, A., Esposito, F., Santangelo, G., Picillo, M., Vitale, C., ... Barone, P. (2015). Resting-state functional connectivity associated with mild cognitive impairment in Parkinson's disease. *Journal of Neurology*, 262(2), 425–434. <https://doi.org/10.1007/s00415-014-7591-5>
- Amend, M., Ionescu, T. M., Di, X., Pichler, B. J., Biswal, B. B., & Wehrl, H. F. (2019). Functional resting-state brain connectivity is accompanied by dynamic correlations of application-dependent 18FFDG PET-tracer fluctuations. *NeuroImage*, 196, 161–172. <https://doi.org/10.1016/j.neuroimage.2019.04.034>
- Arnemann, K. L., Stöber, F., Narayan, S., Rabinovici, G. D., & Jagust, W. J. (2018). Metabolic brain networks in aging and preclinical Alzheimer's disease. *NeuroImage Clinical*, 17, 987–999. <https://doi.org/10.1016/j.nicl.2017.12.037>
- Aschenbrenner, S., Tucha, O., & Lange, K. W. (2001). *RWT Regensburger Wortflüssigkeitstest*. Göttingen: Hogrefe Verlag für Psychologie.
- Baggio, H.-C., Segura, B., Sala-Llonch, R., Martí, M.-J., Valdeorola, F., Compta, Y., ... Junqué, C. (2015). Cognitive impairment and resting-state network connectivity in Parkinson's disease. *Human Brain Mapping*, 36(1), 199–212. <https://doi.org/10.1002/hbm.22622>
- Beck, A. T., Steer, R. A., & Brown, G. K. (1996). *Manual for the beck depression inventory-II*. San Antonio, TX: Psychological Corporation.
- Behzadi, Y., Restom, K., Liu, J., & Liu, T. T. (2007). A component based noise correction method (CompCor) for BOLD and perfusion based fMRI. *NeuroImage*, 37, 90–101.
- Biswal, B. B., Mennes, M., Zuo, X.-N., Gohel, S., Kelly, C., Smith, S. M., ... Milham, M. P. (2010). Toward discovery science of human brain function. *Proceedings of the National Academy of Sciences of the United States of America*, 107(10), 4734–4739. <https://doi.org/10.1073/pnas.0911855107>
- Borghammer, P., Chakravarty, M., Jonsdottir, K. Y., Sato, N., Matsuda, H., Ito, K., ... Gjedde, A. (2010). Cortical hypometabolism and hypoperfusion in Parkinson's disease is extensive: Probably even at early disease stages. *Brain Structure & Function*, 214(4), 303–317. <https://doi.org/10.1007/s00429-010-0246-0>
- Brett, M., Anton, J. L., Valabregue, R., & Poline, J.-B. (2002, June). Region of interest analysis using an SPM toolbox [abstract]. Presented at the 8th International Conference on Functional Mapping of the Human Brain, (Vol. 16, No. 2), Sendai, Japan. Available on CD-ROM in NeuroImage.
- Caso, F., Agosta, F., Inuggi, A., Tomic, A., Stankovic, I., Canu, E., ... Filippi, M. (2013). Dysfunction of the default mode network in early Parkinson's disease: A resting state fMRI study (P06.081). *Neurology*, 80(Suppl. 7), P06.081.
- Clark, C. M., & Stoessl, A. J. (1986). Glucose use correlations: A matter of inference. *Journal of Cerebral Blood Flow & Metabolism*, 6(4), 511–512. <https://doi.org/10.1038/jcbfm.1986.87>
- Conio, B., Martino, M., Magioncalda, P., Escelsior, A., Inglese, M., Amore, M., & Northoff, G. (2020). Opposite effects of dopamine and serotonin on resting-state networks: Review and implications for psychiatric disorders. *Molecular Psychiatry*, 25(1), 82–93. <https://doi.org/10.1038/s41380-019-0406-4>
- Della Rosa, P. A., Cerami, C., Gallivanone, F., Prestia, A., Caroli, A., Castiglioni, I., ... Perani, D. (2014). A standardized 18F-FDG-PET template for spatial normalization in statistical parametric mapping of dementia. *Neuroinformatics*, 12(4), 575–593. <https://doi.org/10.1007/s12021-014-9235-4>
- Di, X., & Biswal, B. B. (2012). Metabolic brain covariant networks as revealed by FDG-PET with reference to resting-state fMRI networks. *Brain Connectivity*, 2(5), 275–283. <https://doi.org/10.1089/brain.2012.0086>
- Emre, M., Aarsland, D., Brown, R., Burn, D. J., Duyckaerts, C., Mizuno, Y., ... Dubois, B. (2007). Clinical diagnostic criteria for dementia associated with Parkinson's disease. *Movement Disorders: Official Journal of the Movement Disorder Society*, 22(12), 1689–1707; quiz 1837. <https://doi.org/10.1002/mds.21507>
- Fahn, S., Elton, R. L., & UPDRS Program Members (1987). Unified Parkinson's disease rating scale. In S. Fahn, C. D. Marsden, M. Goldstein, & D. B. Calne (Eds.), *Recent developments in Parkinson's disease* (Vol. 2, pp. 153–163). Florham Park, NJ: Macmillan Health Care Information.
- Filippi, M., Canu, E., Donzuso, G., Stojkovic, T., Basaia, S., Stankovic, I., ... Agosta, F. (2020). Tracking cortical changes throughout cognitive decline in Parkinson's disease. *Movement Disorders: Official Journal of the Movement Disorder Society*, 35(11), 1987–1998. <https://doi.org/10.1002/mds.28228>
- Folstein, M. F., Folstein, S. E., & McHugh, P. R. (1975). Mini-mental state. *Journal of Psychiatric Research*, 12(3), 189–198. [https://doi.org/10.1016/0022-3956\(75\)90026-6](https://doi.org/10.1016/0022-3956(75)90026-6)
- García-García, D., Clavero, P., Gasca Salas, C., Lamet, I., Arbizu, J., Gonzalez-Redondo, R., ... Rodriguez-Oroz, M. C. (2012). Posterior parietooccipital hypometabolism may differentiate mild cognitive impairment from dementia in Parkinson's disease. *European Journal of Nuclear Medicine and Molecular Imaging*, 39(11), 1767–1777. <https://doi.org/10.1007/s00259-012-2198-5>
- Gardini, S., Venneri, A., Sambataro, F., Cuetos, F., Fasano, F., Marchi, M., ... Caffarra, P. (2015). Increased functional connectivity in the default mode network in mild cognitive impairment: A maladaptive compensatory mechanism associated with poor semantic memory performance. *Journal of Alzheimer's Disease*, 45(2), 457–470. <https://doi.org/10.3233/JAD-142547>
- Glaab, E., Trezzi, J.-P., Greuel, A., Jäger, C., Hodak, Z., Drzezga, A., ... Eggers, C. (2019). Integrative analysis of blood metabolomics and PET brain neuroimaging data for Parkinson's disease. *Neurobiology of Disease*, 124, 555–562. <https://doi.org/10.1016/j.nbd.2019.01.003>
- Goldman, J. G., Williams-Gray, C., Barker, R. A., Duda, J. E., & Galvin, J. E. (2014). The spectrum of cognitive impairment in Lewy body diseases. *Movement Disorders: Official Journal of the Movement Disorder Society*, 29(5), 608–621. <https://doi.org/10.1002/mds.25866>
- Goldman, J. G., Vernaleo, B. A., Camicioli, R., Dahodwala, N., Dobkin, R. D., Ellis, T., ... Simmonds, D. (2018). Cognitive impairment in Parkinson's disease: A report from a multidisciplinary symposium on unmet needs and future directions to maintain cognitive health. *NPJ Parkinson's Disease*, 4, 19. <https://doi.org/10.1038/s41531-018-0055-3>

- Gorges, M., Kunz, M. S., Müller, H.-P., Liepelt-Scarfone, I., Storch, A., Dodel, R., ... Kassubek, J. (2020). Longitudinal brain atrophy distribution in advanced Parkinson's disease: What makes the difference in "cognitive status" converters? *Human Brain Mapping*, 41(6), 1416–1434. <https://doi.org/10.1002/hbm.24884>
- Greuel, A., Trezzi, J.-P., Glaab, E., Ruppert, M. C., Maier, F., Jäger, C., ... Eggers, C. (2020). GBA variants in Parkinson's disease: Clinical, metabolomic, and multimodal neuroimaging phenotypes. *Movement Disorders: Official Journal of the Movement Disorder Society*, 35, 2201–2210. <https://doi.org/10.1002/mds.28225>
- Hammes, J., Theis, H., Giehl, K., Hoenig, M. C., Greuel, A., Tittgemeyer, M., ... van Eimeren, T. (2019). Dopamine metabolism of the nucleus accumbens and fronto-striatal connectivity modulate impulse control. *Brain: A Journal of Neurology*, 142(3), 733–743. <https://doi.org/10.1093/brain/awz007>
- Harris, M. E. (1990). *Wisconsin card sorting test computer version*. Odessa, FL: Psychological Assessment Resources.
- Härting, C., & Wechsler, D. (Eds.). (2000). *Wechsler-Gedächtnistest: revidierte Fassung—WMS-R; Manual; deutsche Adaptation der revidierten Fassung der Wechsler Memory scale* (1st ed.). Bern: Huber.
- Hely, M. A., Reid, W. G. J., Adena, M. A., Halliday, G. M., & Morris, J. G. L. (2008). The Sydney multicenter study of Parkinson's disease: The inevitability of dementia at 20 years. *Movement Disorders: Official Journal of the Movement Disorder Society*, 23(6), 837–844. <https://doi.org/10.1002/mds.21956>
- Hilker, R., Thomas, A. V., Klein, J. C., Weisenbach, S., Kalbe, E., Burghaus, L., ... Heiss, W. D. (2005). Dementia in Parkinson disease: Functional imaging of cholinergic and dopaminergic pathways. *Neurology*, 65(11), 1716–1722. <https://doi.org/10.1212/01.wnl.0000191154.78131.f6>
- Hoehn, M. M., & Yahr, M. D. (1967). Parkinsonism: Onset, progression and mortality. *Neurology*, 17(5), 427–442.
- Hohenfeld, C., Werner, C. J., & Reetz, K. (2018). Resting-state connectivity in neurodegenerative disorders: Is there potential for an imaging biomarker? *NeuroImage Clinical*, 18, 849–870. <https://doi.org/10.1016/j.nicl.2018.03.013>
- Hoogland, J., Boel, J. A., de Bie, R. M. A., Geskus, R. B., Schmand, B. A., Dalrymple-Alford, J. C., ... Geurtsen, G. J. (2017). Mild cognitive impairment as a risk factor for Parkinson's disease dementia. *Movement Disorders: Official Journal of the Movement Disorder Society*, 32(7), 1056–1065. <https://doi.org/10.1002/mds.27002>
- Horwitz, B., Grady, C. L., Schlageter, N. L., Duara, R., & Rapoport, S. I. (1987). Interrelations of regional cerebral glucose metabolic rates in Alzheimer's disease. *Brain Research*, 407(2), 294–306. [https://doi.org/10.1016/0006-8993\(87\)91107-3](https://doi.org/10.1016/0006-8993(87)91107-3)
- Hosokai, Y., Nishio, Y., Hirayama, K., Takeda, A., Ishioka, T., Sawada, Y., ... Mori, E. (2009). Distinct patterns of regional cerebral glucose metabolism in Parkinson's disease with and without mild cognitive impairment. *Movement Disorders: Official Journal of the Movement Disorder Society*, 24(6), 854–862. <https://doi.org/10.1002/mds.22444>
- Huang, C., Mattis, P., Perrine, K., Brown, N., Dhawan, V., & Eidelberg, D. (2008). Metabolic abnormalities associated with mild cognitive impairment in Parkinson disease. *Neurology*, 70(16 Pt 2), 1470–1477. <https://doi.org/10.1212/01.wnl.0000304050.05332.9c>
- Ibarretxe-Bilbao, N., Zarei, M., Junque, C., Marti, M. J., Segura, B., Vendrell, P., ... Tolosa, E. (2011). Dysfunctions of cerebral networks precede recognition memory deficits in early Parkinson's disease. *NeuroImage*, 57(2), 589–597. <https://doi.org/10.1016/j.neuroimage.2011.04.049>
- Kalbe, E., Calabrese, P., Kohn, N., Hilker, R., Riedel, O., Wittchen, H.-U., ... Kessler, J. (2008). Screening for cognitive deficits in Parkinson's disease with the Parkinson neuropsychometric dementia assessment (PANDA) instrument. *Parkinsonism & Related Disorders*, 14(2), 93–101. <https://doi.org/10.1016/j.parkreldis.2007.06.008>
- Kaplan, E. F., Googlass, H., & Weintraub, S. (1983). *The Boston naming test* (2nd ed.). Philadelphia: Lea & Febiger.
- Karunanayaka, P. R., Lee, E.-Y., Lewis, M. M., Sen, S., Eslinger, P. J., Yang, Q. X., & Huang, X. (2016). Default mode network differences between rigidity- and tremor-predominant Parkinson's disease. *Cortex: A Journal Devoted to the Study of the Nervous System and Behavior*, 81, 239–250. <https://doi.org/10.1016/j.cortex.2016.04.021>
- Klein, J. C., Eggers, C., Kalbe, E., Weisenbach, S., Hohmann, C., Vollmar, S., ... Hilker, R. (2010). Neurotransmitter changes in dementia with Lewy bodies and Parkinson disease dementia in vivo. *Neurology*, 74(11), 885–892. <https://doi.org/10.1212/WNL.0b013e3181d55f61>
- Krajcovicova, L., Mikl, M., Marecek, R., & Rektorova, I. (2012). The default mode network integrity in patients with Parkinson's disease is levodopa equivalent dose-dependent. *Journal of Neural Transmission (Vienna, Austria: 1996)*, 119(4), 443–454. <https://doi.org/10.1007/s00702-011-0723-5>
- Langston, J. W., Widner, H., Goetz, C. G., Brooks, D., Fahn, S., Freeman, T., & Watts, R. (1992). Core assessment program for intracerebral transplantations (CAPIT). *Movement Disorders: Official Journal of the Movement Disorder Society*, 7(1), 2–13. <https://doi.org/10.1002/mds.870070103>
- Levy, G., Tang, M.-X., Louis, E. D., Côté, L. J., Alfaró, B., Mejia, H., ... Marder, K. (2002). The association of incident dementia with mortality in PD. *Neurology*, 59(11), 1708–1713. <https://doi.org/10.1212/01.WNL.0000036610.36834.E0>
- Litvan, I., Goldman, J. G., Tröster, A. I., Schmand, B. A., Weintraub, D., Petersen, R. C., ... Emre, M. (2012). Diagnostic criteria for mild cognitive impairment in Parkinson's disease: Movement Disorder Society task force guidelines. *Movement Disorders: Official Journal of the Movement Disorder Society*, 27(3), 349–356. <https://doi.org/10.1002/mds.24893>
- Lopes, R., Delmaire, C., Defebvre, L., Moonen, A. J., Duits, A. A., Hofman, P., ... Dujardin, K. (2017). Cognitive phenotypes in parkinson's disease differ in terms of brain-network organization and connectivity. *Human Brain Mapping*, 38(3), 1604–1621. <https://doi.org/10.1002/hbm.23474>
- Lucas-Jiménez, O., Ojeda, N., Peña, J., Díez-Cirarda, M., Cabrera-Zubizarreta, A., Gómez-Esteban, J. C., ... Ibarretxe-Bilbao, N. (2016). Altered functional connectivity in the default mode network is associated with cognitive impairment and brain anatomical changes in Parkinson's disease. *Parkinsonism & Related Disorders*, 33, 58–64. <https://doi.org/10.1016/j.parkreldis.2016.09.012>
- Lyoo, C. H., Jeong, Y., Ryu, Y. H., Rinne, J. O., & Lee, M. S. (2010). Cerebral glucose metabolism of Parkinson's disease patients with mild cognitive impairment. *European Neurology*, 64(2), 65–73. <https://doi.org/10.1159/000315036>
- Nair, J., Klaassen, A.-L., Arato, J., Vyssotski, A. L., Harvey, M., & Rainer, G. (2018). Basal forebrain contributes to default mode network regulation. *Proceedings of the National Academy of Sciences of the United States of America*, 115(6), 1352–1357. <https://doi.org/10.1073/pnas.1712431115>
- Pappatà, S., Santangelo, G., Aarsland, D., Viciomini, C., Longo, K., Bronnick, K., ... Barone, P. (2011). Mild cognitive impairment in drug-naïve patients with PD is associated with cerebral hypometabolism. *Neurology*, 77(14), 1357–1362. <https://doi.org/10.1212/WNL.0b013e3182315259>
- Passow, S., Specht, K., Adamsen, T. C., Biermann, M., Brekke, N., Craven, A. R., ... Hugdahl, K. (2015). Default-mode network functional connectivity is closely related to metabolic activity. *Human Brain Mapping*, 36(6), 2027–2038. <https://doi.org/10.1002/hbm.22753>
- Polito, C., Berti, V., Ramat, S., Vanzi, E., de Cristofaro, M. T., Pellicanò, G., ... Pupi, A. (2012). Interaction of caudate dopamine depletion and brain metabolic changes with cognitive dysfunction in early Parkinson's disease. *Neurobiology of Aging*, 33(1), 206.e29–206.e39. <https://doi.org/10.1016/j.neurobiolaging.2010.09.004>

- Power, J. D., Schlaggar, B. L., & Petersen, S. E. (2015). Recent progress and outstanding issues in motion correction in resting state fMRI. *NeuroImage*, 105, 536–551. <https://doi.org/10.1016/j.neuroimage.2014.10.044>
- Raichle, M. E., MacLeod, A. M., Snyder, A. Z., ... Gordon, L. (2000). A default mode of brain function. *Proceedings of the National Academy of Sciences of the United States of America*, 98(2), 676–682.
- Ray, N. J., Bradburn, S., Murgatroyd, C., Toseeb, U., Mir, P., Kountouriotis, G. K., ... Grothe, M. J. (2018). In vivo cholinergic basal forebrain atrophy predicts cognitive decline in de novo Parkinson's disease. *Brain: A Journal of Neurology*, 141(1), 165–176. <https://doi.org/10.1093/brain/aww310>
- Riedl, V., Bienkowska, K., Strobel, C., Tahmasian, M., Grimmer, T., Förster, S., ... Drzezga, A. (2014). Local activity determines functional connectivity in the resting human brain: A simultaneous FDG-PET/fMRI study. *The Journal of Neuroscience: The Official Journal of the Society for Neuroscience*, 34(18), 6260–6266. <https://doi.org/10.1523/JNEUROSCI.0492-14.2014>
- Ruppert, M. C., Greuel, A., Tahmasian, M., Schwartz, F., Stürmer, S., Maier, F., ... Eggers, C. (2020). Network degeneration in Parkinson's disease: Multimodal imaging of nigro-striato-cortical dysfunction. *Brain: A Journal of Neurology*, 143(3), 944–959. <https://doi.org/10.1093/brain/awaa019>
- Sala, A., & Perani, D. (2019). Brain molecular connectivity in neurodegenerative diseases: Recent advances and new perspectives using positron emission tomography. *Frontiers in Neuroscience*, 13, 617. <https://doi.org/10.3389/fnins.2019.00617>
- Sala, A., Caminiti, S. P., Presotto, L., Premi, E., Pilotto, A., Turrone, R., ... Perani, D. (2017). Altered brain metabolic connectivity at multiscale level in early Parkinson's disease. *Scientific Reports*, 7(1), 4256. <https://doi.org/10.1038/s41598-017-04102-z>
- Savio, A., Fänger, S., Tahmasian, M., Rachakonda, S., Manoliu, A., Sorg, C., ... Yakushev, I. (2017). Resting-state networks as simultaneously measured with functional MRI and PET. *Journal of Nuclear Medicine: Official Publication, Society of Nuclear Medicine*, 58(8), 1314–1317. <https://doi.org/10.2967/jnumed.116.185835>
- Spetsieris, P. G., Ko, J. H., Tang, C. C., Nazem, A., Sako, W., Peng, S., ... Eidelberg, D. (2015). Metabolic resting-state brain networks in health and disease. *Proceedings of the National Academy of Sciences of the United States of America*, 112(8), 2563–2568. <https://doi.org/10.1073/pnas.1411011112>
- Tahmasian, M., Bettray, L. M., van Eimeren, T., Drzezga, A., Timmermann, L., Eickhoff, C. R., ... Eggers, C. (2015). A systematic review on the applications of resting-state fMRI in Parkinson's disease: Does dopamine replacement therapy play a role? *Cortex; A Journal Devoted to the Study of the Nervous System and Behavior*, 73, 80–105. <https://doi.org/10.1016/j.cortex.2015.08.005>
- Tahmasian, M., Eickhoff, S. B., Giehl, K., Schwartz, F., Herz, D. M., Drzezga, A., ... Eickhoff, C. R. (2017). Resting-state functional reorganization in Parkinson's disease: An activation likelihood estimation meta-analysis. *Cortex; A Journal Devoted to the Study of the Nervous System and Behavior*, 92, 119–138. <https://doi.org/10.1016/j.cortex.2017.03.016>
- Tessitore, A., Esposito, F., Vitale, C., Santangelo, G., Amboni, M., Russo, A., ... Tedeschi, G. (2012). Default-mode network connectivity in cognitively unimpaired patients with Parkinson disease. *Neurology*, 79(23), 2226–2232. <https://doi.org/10.1212/WNL.0b013e31827689d6>
- Tomlinson, C. L., Stowe, R., Patel, S., Rick, C., Gray, R., & Clarke, C. E. (2010). Systematic review of levodopa dose equivalency reporting in Parkinson's disease. *Movement Disorder Society*, 25(15), 2649–2653. <https://doi.org/10.1002/mds.23429>
- Toussaint, P.-J., Perlberg, V., Bellec, P., Desarnaud, S., Lacomblez, L., Doyon, J., ... Benali, H. (2012). Resting state FDG-PET functional connectivity as an early biomarker of Alzheimer's disease using conjoint univariate and independent component analyses. *NeuroImage*, 63(2), 936–946. <https://doi.org/10.1016/j.neuroimage.2012.03.091>
- van Eimeren, T., Monchi, O., Ballanger, B., & Strafella, A. P. (2009). Dysfunction of the default mode network in Parkinson disease: A functional magnetic resonance imaging study. *Archives of Neurology*, 66(7), 877–883. <https://doi.org/10.1001/archneurol.2009.97>
- Wehrl, H. F., Hossain, M., Lankes, K., Liu, C.-C., Bezrukov, I., Martirosian, P., ... Pichler, B. J. (2013). Simultaneous PET-MRI reveals brain function in activated and resting state on metabolic, hemodynamic and multiple temporal scales. *Nature Medicine*, 19(9), 1184–1189. <https://doi.org/10.1038/nm.3290>
- Williams-Gray, C. H., Evans, J. R., Goris, A., Foltynie, T., Ban, M., Robbins, T. W., ... Barker, R. A. (2009). The distinct cognitive syndromes of Parkinson's disease: 5 year follow-up of the CamPaIGN cohort. *Brain: A Journal of Neurology*, 132(Pt 11), 2958–2969. <https://doi.org/10.1093/brain/awp245>
- Win, T. P., Hosokai, Y., Minagawa, T., Muroi, K., Miwa, K., Maruyama, A., ... Saito, H. (2019). Comparison of count normalization methods for statistical parametric mapping analysis using a digital brain phantom obtained from Fluorodeoxyglucose-positron emission tomography. *Asia Oceania Journal of Nuclear Medicine & Biology*, 7(1), 58–70. <https://doi.org/10.22038/AOJNMB.2018.11745>
- Yakushev, I., Hammers, A., Fellgiebel, A., Schmidtman, I., Scheurich, A., Buchholz, H.-G., ... Schreckenberger, M. (2009). Spm-based count normalization provides excellent discrimination of mild Alzheimer's disease and amnesic mild cognitive impairment from healthy aging. *NeuroImage*, 44(1), 43–50. <https://doi.org/10.1016/j.neuroimage.2008.07.015>
- Yakushev, I., Chételat, G., Fischer, F. U., Landeau, B., Bastin, C., Scheurich, A., ... Salmon, E. (2013). Metabolic and structural connectivity within the default mode network relates to working memory performance in young healthy adults. *NeuroImage*, 79, 184–190. <https://doi.org/10.1016/j.neuroimage.2013.04.069>
- Zhan, Z.-W., Lin, L.-Z., Yu, E.-H., Xin, J.-W., Lin, L., Lin, H.-L., ... Pan, X.-D. (2018). Abnormal resting-state functional connectivity in posterior cingulate cortex of Parkinson's disease with mild cognitive impairment and dementia. *CNS Neuroscience & Therapeutics*, 24(10), 897–905. <https://doi.org/10.1111/cns.12838>
- Zou, K. H., Warfield, S. K., Bharatha, A., Tempany, C. M. C., Kaus, M. R., Haker, S. J., ... Kikinis, R. (2004). Statistical validation of image segmentation quality based on a spatial overlap index1. *Academic Radiology*, 11(2), 178–189. [https://doi.org/10.1016/S1076-6332\(03\)00671-8](https://doi.org/10.1016/S1076-6332(03)00671-8)

SUPPORTING INFORMATION

Additional supporting information may be found online in the Supporting Information section at the end of this article.

How to cite this article: Ruppert MC, Greuel A, Freigang J, et al. The default mode network and cognition in Parkinson's disease: A multimodal resting-state network approach. *Hum Brain Mapp*. 2021;42:2623–2641. <https://doi.org/10.1002/hbm.25393>